

Vinod K. Misra,<sup>1</sup>

Ross Shiman,<sup>2</sup>

David E. Draper<sup>2</sup>

<sup>1</sup> Department of Chemistry  
and Department of Pediatrics  
Medical Genetics  
The University of Michigan  
1924 Taubman Center  
1500 E. Medical Center Drive  
Ann Arbor, MI 48109-0318

<sup>2</sup> Department of Chemistry  
The Johns Hopkins University  
3400 N. Charles Street  
Baltimore, MD 21218

Received 6 November 2002;  
accepted 7 November 2002

---

## A Thermodynamic Framework for the Magnesium-Dependent Folding of RNA

**Abstract:** The goal of this review is to present a unified picture of the relationship between ion binding and RNA folding based on recent theoretical and computational advances. In particular, we present a model describing how the association of magnesium ions is coupled to the tertiary structure folding of several well-characterized RNA molecules. This model is developed in terms of the nonlinear Poisson–Boltzmann (NLPB) equation, which provides a rigorous electrostatic description of the interaction between  $Mg^{2+}$  and specific RNA structures. In our description, most of the ions surrounding an RNA behave as a thermally fluctuating ensemble distributed according to a Boltzmann weighted average of the mean electrostatic potential around the RNA. In some cases, however, individual ions near the RNA may shed some of their surrounding waters to optimize their Coulombic interactions with the negatively charged ligands on the RNA. These chelated ions are energetically distinct from the surrounding ensemble and must be treated explicitly. This model is used to explore several different RNA systems that interact differently with  $Mg^{2+}$ . In each case, the NLPB equation accurately describes the stoichiometric and energetic linkage between  $Mg^{2+}$  binding and RNA folding without requiring any fitted parameters in the calculation. Based on this model, we present a physical description of how  $Mg^{2+}$  binds and stabilizes specific RNA structures to promote the folding reaction. © 2003 Wiley Periodicals, Inc. *Biopolymers* 69: 118–136, 2003

**Keywords:** ion binding; RNA folding; magnesium; tertiary structure; nonlinear Poisson–Boltzmann equation; electrostatics

---

Correspondence to: David E. Draper; email: draper@jhunix.hcf.jhu.edu or Vinod K. Misra; email: vmisra@umich.edu

Contract grant sponsor: Howard Hughes Medical Institute and NIHS

Contract grant number: GM58545 (NIH)

*Biopolymers*, Vol. 69, 118–136 (2003)

© 2003 Wiley Periodicals, Inc.

## INTRODUCTION

Ribonucleic acids (RNAs) fold into a variety of complex structures<sup>1,2</sup> that are required for their many biological activities.<sup>3</sup> Thus, appreciating RNA function requires knowledge of the forces responsible for the underlying RNA structures. However, understanding just how an extended chain of negatively charged nucleotides collapses into a compact functional structure remains an unresolved problem. Since the strong electrostatic repulsion among the closely packed, negatively charged phosphate groups on the RNA backbone tends to disrupt the folded structure, an important facet to the RNA folding problem is understanding how these repulsions are compensated in the folded state. Although monovalent cations can effectively reduce these repulsions and stabilize the folded structure of many RNA molecules,<sup>4–8</sup> the unique role of divalent cations, like magnesium, has always been evident.  $Mg^{2+}$  strongly stabilizes the native tertiary structure of most RNAs and favors the folding reaction, even in the presence of a large excess of monovalent ions.<sup>4</sup>

The goal of this review is to present a unified picture of the relationship between ion binding and RNA folding based on recent theoretical and computational advances. In particular, we have developed a theoretical model based on the nonlinear Poisson–Boltzmann (NLPB) equation to describe how  $Mg^{2+}$  binds and stabilizes specific RNA structures.<sup>9–11</sup> This model is presented here to describe the linkage between the association of magnesium ions and folding of tertiary structure for several different RNA systems.

## A DESCRIPTION OF MAGNESIUM BINDING TO RNA

### The Linkage Between $Mg^{2+}$ Interactions and RNA Folding

In many cases, RNA folding can be described as a stepwise process that proceeds through increasingly organized intermediate states.<sup>12–14</sup> Fully denatured RNAs exist in an unfolded state best characterized as an extended chain with little or no defined secondary structure. The initial stages of RNA folding lead to a compact, disordered intermediate state, designated I,<sup>15–17</sup> characterized by elements of helical secondary structure without well-defined tertiary contacts. As folding proceeds, the secondary structural elements of the I state assemble into compact domains of tertiary

structure that associate to form the native tertiary structure, designated N.

The folding of tertiary structure can be described by the equilibrium,



The apparent equilibrium constant for this reaction,  $K_F^{\text{app}}$ , is a magnesium concentration dependent term that can be written<sup>18</sup>

$$K_F^{\text{app}} = \xi_N / \xi_I \quad (2)$$

where  $\xi_I$  and  $\xi_N$  are the partition functions for the association of  $Mg^{2+}$  with the I and N forms of the RNA, respectively.

The linkage between tertiary structure folding and magnesium ion association can be described by the thermodynamic cycle in Figure 1. In this cycle, we define the term  $\Delta\Delta G_F$  as follows:

$$\Delta\Delta G_F = \Delta G_F^{\text{Mg}} - \Delta G_F^{\circ} = -kT \ln(K_F^{\text{app}}) \quad (3)$$

where the terms  $\Delta G_F^{\text{Mg}}$  and  $\Delta G_F^{\circ}$  are the free energies of RNA folding in the presence and absence of magnesium, respectively.  $\Delta\Delta G_F$  is the free energy contribution of the added magnesium salt to the RNA folding reaction. The terms  $\Delta G_{\text{Mg}}^{\text{N}} = -kT \ln(\xi_N)$  and  $\Delta G_{\text{Mg}}^{\text{I}} = -kT \ln(\xi_I)$  are the free energies of magnesium binding to the N and I states, respectively. The differences between  $\Delta G_F^{\text{Mg}}$  and  $\Delta G_F^{\circ}$  is equal to the difference between  $\Delta G_{\text{Mg}}^{\text{N}}$  and  $\Delta G_{\text{Mg}}^{\text{I}}$ .

$$\Delta\Delta G_F = \Delta G_F^{\text{Mg}} - \Delta G_F^{\circ} = \Delta G_{\text{Mg}}^{\text{N}} - \Delta G_{\text{Mg}}^{\text{I}} = \Delta\Delta G_{\text{Mg}} \quad (4)$$

The term  $\Delta\Delta G_{\text{Mg}}$  is the difference in the  $Mg^{2+}$  interaction free energy between the N and I states. The value of  $\Delta\Delta G_{\text{Mg}}$  is often experimentally determined by measuring  $\Delta\Delta G_F$  using experimental techniques like thermal denaturation.<sup>19,20</sup> Conceptually, however, understanding why the free energy of RNA folding in the presence of  $Mg^{2+}$  ( $\Delta G_F^{\text{Mg}}$ ) is more favorable than in its absence ( $\Delta G_F^{\circ}$ ), requires an understanding of why the free energy of  $Mg^{2+}$  interactions with the folded state ( $\Delta G_{\text{Mg}}^{\text{N}}$ ) are so much more favorable than to the partially unfolded intermediate state, I ( $\Delta G_{\text{Mg}}^{\text{I}}$ ).

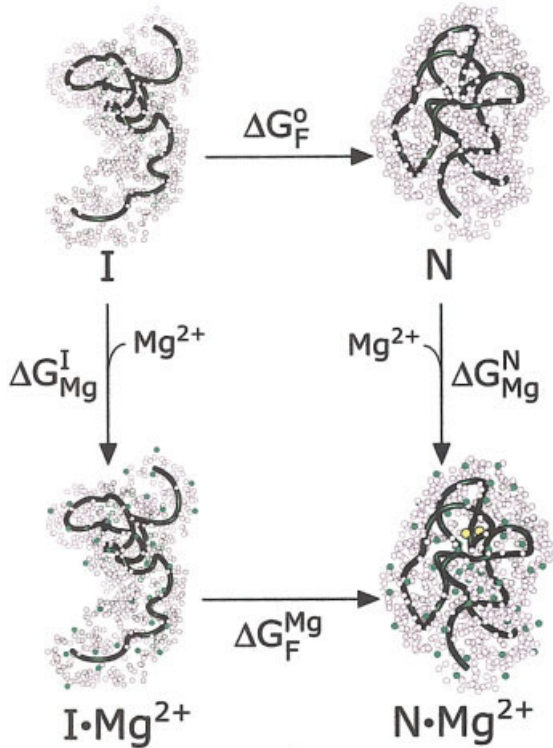


**FIGURE 1** The thermodynamic cycle describing the relationship between  $\text{Mg}^{2+}$  binding and RNA folding. The tertiary folding reaction is an equilibrium between an intermediate (I) state and a folded (N) state, involving compaction of secondary structure into tertiary structure, as described in the text. The reaction occurs in a solution containing a fixed concentration of monovalent cations, shown as small gray spheres. Folding is characterized by the free energies  $\Delta G_F^0$  and  $\Delta G_F^{\text{Mg}}$  in the presence and absence of  $\text{Mg}^{2+}$ , respectively.  $\text{Mg}^{2+}$  that are part of the surrounding electrostatic ensemble are shown as small green spheres, while specifically chelated  $\text{Mg}^{2+}$  are shown as yellow spheres. The interactions of  $\text{Mg}^{2+}$  with the I and N states are described by the free energies  $\Delta G_{\text{Mg}}^{\text{I}}$  and  $\Delta G_{\text{Mg}}^{\text{N}}$ , respectively. The molecular states that interact with Mg ions are designated  $\text{I} \cdot \text{Mg}^{2+}$  and  $\text{N} \cdot \text{Mg}^{2+}$ . The free energy contribution of  $\text{Mg}^{2+}$  to the tertiary folding reaction is  $\Delta \Delta G_{\text{Mg}} = \Delta G_{\text{Mg}}^{\text{N}} - \Delta G_{\text{Mg}}^{\text{I}}$ .

### A Thermodynamic Description of $\text{Mg}^{2+}$ Binding

The interactions of the alkaline group I and II metal ions with nucleic acids are governed by their strong electrostatic attraction to the negatively charged phosphodiester backbone. As a result, RNAs are surrounded by a group of ions whose charge is equal and opposite to that of the RNA. The macroscopically observed stabilization free energy of an RNA by added salt arises from the interaction of the entire group of ions surrounding the RNA with the electro-

static field. However, the thermodynamic properties of an individual ion near the RNA cannot be determined independently of its interactions with other ions; this interdependence among surrounding charges is referred to as electrostatic coupling.

A useful way to think about the association of ions with an RNA is in terms of the thermodynamic properties of the macromolecule. In such a description, ionic association is manifested by a change in the activity coefficient of the RNA upon adding salt to an aqueous solution.<sup>21,22</sup> In this formalism, the chemical potential of the RNA,  $\mu_{\text{RNA}}$ , can be written<sup>23</sup>

$$\begin{aligned} \mu_{\text{RNA}} &= \mu_{\text{RNA}}^{\circ} + kT \ln(a_{\text{RNA}}) \\ &= \mu_{\text{RNA}}^{\circ} + kT \ln(\gamma_{\text{RNA}} c_{\text{RNA}}) \end{aligned} \quad (5)$$

where  $a_{\text{RNA}}$  is the activity of the RNA with concentration  $c_{\text{RNA}}$  in a salt containing solution; and  $\mu_{\text{RNA}}^{\circ}$  is the standard state chemical potential of the RNA in the absence of any salt. The activity coefficient,  $\gamma_{\text{RNA}}$ , is directly related to the excess electrostatic free energy of the RNA relative to the standard state. The term  $\gamma_{\text{RNA}}$  accounts for all of the thermodynamic interactions of the added salt with the RNA. We note that  $\gamma_{\text{RNA}}$  goes to unity in the limit of infinite salt dilution (pure aqueous solution).<sup>23</sup> Practically, the interaction free energy,  $\Delta G_{\text{Mg}}$ , of added magnesium chloride with an RNA is given by

$$\Delta G_{\text{Mg}} = \mu_{\text{RNA}}(2) - \mu_{\text{RNA}}(1) = kT \ln(\gamma_{\text{RNA}}(2)/\gamma_{\text{RNA}}(1)) \quad (6)$$

where  $\mu_{\text{RNA}}(2)$  is the chemical potential of the RNA in a solution containing the added salt of interest (e.g., containing  $\text{MgCl}_2$  and  $\text{NaCl}$ ) and  $\mu_{\text{RNA}}(1)$  is the chemical potential in a reference solution (e.g., containing only  $\text{NaCl}$ );  $\gamma_{\text{RNA}}(2)$  and  $\gamma_{\text{RNA}}(1)$  are the corresponding activity coefficients. Any ions that perturb the activity coefficient of the RNA relative to the standard state are said to be “thermodynamically bound” to the RNA. Thus, the term  $\Delta G_{\text{Mg}}$  for a particular RNA conformation (e.g., the N or I state) reflects the extent to which thermodynamically bound magnesium ions affect  $\gamma_{\text{RNA}}$ .  $\Delta G_{\text{Mg}}$  is directly related to the partition function for  $\text{Mg}^{2+}$  binding to that state, as noted above.

The stoichiometry of thermodynamic ion binding can be determined experimentally from the Donnan coefficient (or preferential interaction coefficient),  $\Gamma_s$ , of the RNA.<sup>21,24</sup> Thus, for  $\text{MgCl}_2$

$$\Gamma_s = \frac{\partial(\Delta G_{\text{Mg}}/kT)}{\partial \ln(c_{\text{Mg}})} \quad (7)$$

where  $c_{\text{Mg}}$  is the bulk concentration of  $\text{MgCl}_2$ . The Donnan coefficient describes the distribution of ions across a semipermeable membrane in an equilibrium dialysis experiment. The value of  $\Gamma_s$  for nucleic acids is sometimes estimated from the experimentally measured fraction of bound cations. However, it is important to realize that this ignores potentially important thermodynamic contributions of coions added as part of the magnesium salt.<sup>9</sup> Alternatively, the change in the Donnan coefficient associated with a folding transition,  $\Delta\Gamma_s$ , can be measured from the salt dependence of  $K_F^{\text{app}}$ . For example, the thermodynamic uptake of  $\text{MgCl}_2$  upon RNA folding,  $\Delta\Gamma_{\text{MgCl}_2}$ , is given by

$$\begin{aligned} \Delta\Gamma_{\text{MgCl}_2} &= \frac{\partial \ln(K_F^{\text{app}})}{\partial \ln(c_{\text{Mg}})} = \frac{\partial(\Delta G_{\text{Mg}}^{\text{N}}/kT)}{\partial \ln(c_{\text{Mg}})} - \frac{\partial(\Delta G_{\text{Mg}}^{\text{I}}/kT)}{\partial \ln(c_{\text{Mg}})} \\ &= \Gamma_{\text{MgCl}_2}^{\text{N}} - \Gamma_{\text{MgCl}_2}^{\text{I}} \quad (8) \end{aligned}$$

For many RNA systems,  $K_F^{\text{app}}$  is not measured directly; rather, the probability for observing the folded state,  $p_{\text{N}}$ , is measured as a function of magnesium concentration using methods like hydroxyl radical protection, circular dichroism, or fluorescence spectroscopy.<sup>25</sup> The term  $p_{\text{N}}$  is related to  $K_F^{\text{app}}$  by the following relationship<sup>28</sup>:

$$p_{\text{N}} = \frac{[\text{N}]}{[\text{N}] + [\text{I}]} = \frac{K_F^{\text{app}}}{1 + K_F^{\text{app}}} = \frac{\xi_{\text{N}}}{\xi_{\text{N}} + \xi_{\text{I}}} \quad (9)$$

At the transition midpoint of the folding reaction (where  $p_{\text{N}} = 0.5$  and  $K_F^{\text{app}} = 1$ ), it can be shown that<sup>28</sup>

$$\left( \frac{\partial p_{\text{N}}}{\partial \ln(c_{\text{Mg}})} \right)_{p_{\text{N}}=0.5} = \frac{1}{4} (\Delta\Gamma_{\text{MgCl}_2}) \quad (10)$$

The term  $\Delta\Gamma_{\text{MgCl}_2}$  is equivalent to the Hill coefficient under these conditions.<sup>28</sup> However, we note that  $\Delta\Gamma_{\text{MgCl}_2}$  depends on both  $\text{NaCl}$  and  $\text{MgCl}_2$  concentrations. A proper physical interpretation of the experimental data requires a quantitative model describing the partition functions for magnesium binding to the unfolded and folded states,  $\xi_{\text{I}}$  and  $\xi_{\text{N}}$ , that accounts for the electrostatic coupling among all the ions in solution.

## A Theoretical Description of $\text{Mg}^{2+}$ Binding

The classical treatment of the electrostatic interactions among charges in a salt-containing solution is based on the Poisson–Boltzmann (PB) equation,<sup>22,29</sup>

$$\begin{aligned} \nabla \cdot [\varepsilon(\mathbf{r})\nabla \cdot \phi(\mathbf{r})] + 4\pi\rho^{\text{f}}(\mathbf{r}) \\ + 4\pi \sum_i (c_i Z_i e) \exp\left(\frac{-Z_i e \phi(\mathbf{r})}{kT}\right) = 0 \quad (11) \end{aligned}$$

in which  $\phi$  is the electrostatic potential,  $\varepsilon$  is the dielectric constant; and  $\rho^{\text{f}}$  is the fixed charge density (arising from charges on the RNA),  $c_i$  is the bulk concentration and ionic species  $i$ ,  $Z_i$  is the valence of  $i$ ,  $k$  is Boltzmann's constant,  $T$  is the absolute temperature and  $e$  is the proton charge. The quantities  $\phi$ ,  $\varepsilon$ , and  $\rho$  are all functions of the position vector  $\mathbf{r}$  in the reference frame centered on a fixed macromolecule.

In this model, ions surrounding an RNA behave as a thermally fluctuating ensemble distributed according to a Boltzmann weighted average of the mean electrostatic potential around the RNA [given by the third term in Eq. (11)]. The ensemble treatment makes two key assumptions about the surrounding ions: first, the ions only interact with the nucleic acid via long-range Coulombic interactions; and second, on average, each ion's hydration layer remains intact. Importantly, the ensemble description implicitly accounts for the strongly coupled electrostatic interactions of each ionic species with the RNA. Accounting for the electrostatic coupling among ions is crucial for a proper physical description of ionic interactions with RNA as shown below.

Individual ions within the ensemble surrounding the RNA diffuse through space under the influence of the electrostatic field. As implied by the Boltzmann distribution, the probability of finding an ion in a given region of space is proportional to the electrostatic potential there. As such, high concentrations of these ions are found in deep pockets of negative electrostatic potential formed by the irregular shape of the molecular surface. It is these highly localized ions that are often detected by experimental methods like NMR or x-ray crystallography.<sup>10,30</sup> However, since the ions are all electrostatically coupled, the thermodynamic properties of these individual ions cannot be uniquely determined. Rather, the equilibrium thermodynamic properties of these ions can only be determined as part of an ensemble average of all the monovalent and divalent cations and anions (e.g.,  $\text{Na}^+$ ,  $\text{Mg}^{2+}$ ,  $\text{Cl}^-$ , etc.) surrounding the RNA.

In some cases, however, individual Mg ions near the RNA may shed some of their surrounding waters to optimize their Coulombic interactions with the negatively charged ligands on the RNA. For example, specific ions can be chelated by anionic RNA ligands positioned by tertiary structure folding. However, the energetic cost of perturbing waters around these Mg ions is large. In the extreme case, completely remov-

ing a Mg ion from water costs nearly  $460 \text{ kcal} \cdot \text{mol}^{-1}$ .<sup>31</sup> Removal of all the outer water molecules, leaving just the inner hydration layer intact, costs more than  $200 \text{ kcal} \cdot \text{mol}^{-1}$  and removal of only one of these outer-layer water molecules can cost up to  $10 \text{ kcal} \cdot \text{mol}^{-1}$ .<sup>32</sup> The removal of a single water molecule from the inner hydration layer costs more than  $30 \text{ kcal} \cdot \text{mol}^{-1}$ .<sup>32</sup>

The large cost of dehydration for these chelated ions must be compensated by other favorable interactions. The balance between ionic attraction and dehydration is the basis for the characteristic selectivity of a site for particular ions, as suggested by Eisenman nearly 40 years ago.<sup>33,34</sup> The Eisenman hypothesis is that the binding process can be broken down into two steps: first, stripping water molecules away from the ion, and second, bringing the ion into contact with the negative charges at the site. The basic point of Eisenman's proposal is that, for favorable binding, the electrostatic attraction of an ion to its site must outweigh the large cost of dehydration.

Since the ensemble description does not adequately treat the large free energies associated with chelation, both the Coulombic interactions and the ionic dehydration for these ions must be explicitly treated. Coulombic interactions between the ion and the RNA can be calculated explicitly knowing the positions of the charges.<sup>35</sup> However, these calculations must also account for the electrostatic coupling between the explicitly treated ion and the surrounding ionic ensemble. The desolvation of the bound ion can be simply treated using the Born model, which has been applied in the context of the nonlinear Poisson–Boltzmann (NLPB) model to treat  $\text{Mg}^{2+}$  chelated by RNA.<sup>11</sup> In the next section, an overall model for ionic association with RNA is developed in terms of a theoretical model based on the NLPB equation. This model will formally account for energetically different modes of binding.

## A Quantitative Model for $\text{Mg}^{2+}$ Binding

The chemical potential of an RNA molecule in an aqueous solution containing  $\text{MgCl}_2$  and  $\text{NaCl}$  can be written as<sup>4,23</sup>

$$\mu_{\text{RNA}} = \mu_{\text{RNA}}^{\circ}(v) + \Delta G_{\text{RNA}}^{v \rightarrow w} + \Delta G_{\text{RNA}}^{w \rightarrow s_1} + \Delta G_{\text{RNA}}^{s_1 \rightarrow s_2} + kT \ln c_{\text{RNA}} \quad (12)$$

where  $k$  is the Boltzmann constant;  $T$  is the absolute temperature;  $c_{\text{RNA}}$  is the molar concentration of the RNA in a particular folded state; the term  $\mu_{\text{RNA}}^{\circ}(v)$  is the vacuum standard state chemical potential;

$\Delta G_{\text{RNA}}^{v \rightarrow w}$ ,  $\Delta G_{\text{RNA}}^{w \rightarrow s_1}$ , and  $\Delta G_{\text{RNA}}^{s_1 \rightarrow s_2}$  are the free energies of transferring the RNA molecule from vacuum to pure water, from pure water to a univalent salt solution, and from the univalent salt solution to a mixed salt solution (containing both  $\text{MgCl}_2$  and  $\text{NaCl}$ ), respectively. Focusing on the interaction of divalent ions with the RNA, a reference state containing an arbitrary concentration of monovalent salt is defined as

$$\mu_{\text{RNA}}^{\circ}(s_1) = \mu_{\text{RNA}}^{\circ}(v) + \Delta G_{\text{RNA}}^{v \rightarrow w} + \Delta G_{\text{RNA}}^{w \rightarrow s_1} + kT \ln c_{\text{RNA}} \quad (13)$$

so that the overall chemical potential of the RNA can then be written

$$\mu_{\text{RNA}} = \mu_{\text{RNA}}^{\circ}(s_1) + \Delta G_{\text{RNA}}^{s_1 \rightarrow s_2} \quad (14)$$

The last term,  $\Delta G_{\text{RNA}}^{s_1 \rightarrow s_2}$ , includes contributions from all the magnesium ions within the surrounding ensemble as well as ions chelated by the RNA. For consistency with our previous discussion, the shorthand notation of  $\Delta G_{\text{Mg}}$  will refer to  $\Delta G_{\text{RNA}}^{s_1 \rightarrow s_2}$ .

Figure 2 shows a thermodynamic pathway for partitioning  $\Delta G_{\text{Mg}}$  into contributions from both implicitly treated ions that are part of the surrounding ensemble as well as explicitly treated ions that are chelated by the RNA. In this pathway, the initial state is simply the RNA in a reference state univalent salt solution. The chemical potential of the RNA in this state is given by  $\mu_{\text{RNA}}^{\circ}(s_1)$ , defined above. In the first step, the RNA is transferred into a solution containing the reference state concentration of monovalent salt (e.g.,  $\text{NaCl}$ ) along with a fixed concentration of  $\text{MgCl}_2$ . The free energy of this step,  $\Delta G_{\text{D}}$  (where the subscript “D” refers to ions that are described as “distribution”), is defined as the interaction of the RNA with the  $\text{MgCl}_2$  ensemble that is treated using a distribution function determined by the surrounding electrostatic potentials. In the second step, chelated Mg ions bind to specific locations on the RNA in the presence of the ensembles of monovalent and divalent cations. The free energy of this step is given by  $\Delta G_{\text{S}}$  (where the subscript “S” refers to ions that are explicitly treated at specific “sites”). The overall magnesium binding free energy,  $\Delta G_{\text{Mg}}$ , is

$$\Delta G_{\text{Mg}} = \Delta G_{\text{D}} + \Delta G_{\text{S}} \quad (15)$$

These free energy terms are discussed in more detail below.

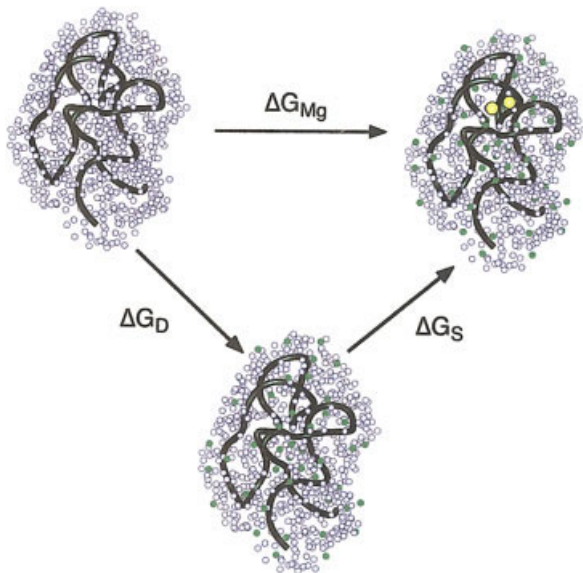


**FIGURE 2** The thermodynamic pathway for calculating the interaction  $\text{Mg}^{2+}$  with a given conformational state of RNA,  $\Delta G_{\text{Mg}}$ . This process consists of the free energy of chelation to a specific site,  $\Delta G_{\text{S}}$ , and the association of the surrounding  $\text{Mg}^{2+}$  ensemble with the RNA,  $\Delta G_{\text{D}}$ . The small green spheres represent  $\text{Mg}^{2+}$  that interact as part of the ensemble; the yellow spheres represent chelated  $\text{Mg}^{2+}$ . Again, the reaction occurs in a solution containing a fixed concentration of monovalent cations, shown as small gray spheres.

**The Interaction of the  $\text{Mg}^{2+}$  Ensemble with the RNA.** The term  $\Delta G_{\text{D}}$  is the free energy of assembling a thermodynamically bound ensemble of Mg ions around the RNA. In the NLPB formalism, the ensemble of Mg ions is treated as a cosolvent that affects the equilibrium through its influence on the chemical potential (or activity coefficients) of the RNA.<sup>36</sup> This treatment is noteworthy since the long-range electrostatic interactions among ions in solution cannot be described properly by a simple mass action relationship.

The term  $\Delta G_{\text{D}}$ , shown in Figure 2, is determined by the difference between the electrostatic free energy of the RNA (without any chelated ions) in a magnesium containing solution [ $\Delta G_{\text{el}}(\text{Mg})$ ] and a magnesium free solution [ $\Delta G_{\text{el}}(\text{Mg} = 0)$ ], so that

$$\Delta G_{\text{D}} = \Delta G_{\text{el}}(\text{Mg}) - \Delta G_{\text{el}}(\text{Mg} = 0) \quad (16)$$

In the NLPB model, the electrostatic free energy,  $\Delta G_{\text{el}}$ , of the RNA in an aqueous solution containing NaCl and  $\text{MgCl}_2$  can be written as the sum of three terms<sup>29,37</sup>

$$\Delta G_{\text{el}} = \Delta G_{\text{E-D}} + \Delta G_{\text{org}}^{\text{Na}} + \Delta G_{\text{org}}^{\text{Mg}} \quad (17)$$

given by the three integrals over all space ( $r$ ):

$$\Delta G_{\text{E-D}} = \int \frac{\rho(r)\phi(r)}{2} dr \quad (18)$$

$$\Delta G_{\text{org}}^{\text{Na}} = \int [-\rho_{\text{Na}}(r)\phi(r) - kTc_{\text{Na}}(e^{-\phi(r)} + e^{\phi(r)} - 2)]dr \quad (19)$$

$$\Delta G_{\text{org}}^{\text{Mg}} = \int [-\rho_{\text{Mg}}(r)\phi(r) - kTc_{\text{Mg}}(e^{-2\phi(r)} + 2e^{\phi(r)} - 3)]dr \quad (20)$$

in which the energies are given in units of  $kT$ . The term  $\rho(r)$  is the total charge density arising from the fixed (RNA) charges and the mobile ions (e.g., NaCl and  $\text{MgCl}_2$ ) at a given point in space;  $\phi(r)$  is the reduced electrostatic potential [ $e\psi(r)/kT$ , where  $e$  is the protonic charge,  $k$  is the Boltzmann constant;  $T$  is the absolute temperature;  $\psi(r)$  is the electrostatic potential at position ( $r$ )]; and  $c_{\text{Na}}$  and  $c_{\text{Mg}}$  are the bulk sodium and magnesium ion concentrations, respectively. The term  $\Delta G_{\text{E-D}}$  is the electrostatic stress of the system, which represents the free energy of the Coulombic interactions among all charges in the system (e.g., nucleic acid phosphates, partially charged RNA moieties,  $\text{Na}^+$ ,  $\text{Mg}^{2+}$ , and  $\text{Cl}^-$ ). The terms  $\Delta G_{\text{org}}^{\text{Na}}$  and  $\Delta G_{\text{org}}^{\text{Mg}}$  are the entropic free energies of assembling the ensemble of NaCl and  $\text{MgCl}_2$  around the nucleic acid, respectively.<sup>29</sup>

In the ensemble description, the number of bound ions for the species  $i$  is calculated by integrating the number of ions that are associated with the nucleic acid over all space:

$$\nu_i = \int [c_i(e^{-z\phi(r)} - 1)] dr \quad (21)$$

The term  $\nu_i$  is, therefore, the thermodynamically bound fraction of a  $z$ -valent,  $i$ , around the nucleic acid relative to its bulk concentration,  $c_i$ .<sup>38</sup> The value of  $\nu_{\text{Mg}}$  is sometimes experimentally determined and can be compared directly to calculated values of the excess accumulation of bound magnesium ions using Eq. (21). However, in many cases, it is actually the preferential interaction coefficient of the ensemble,  $\Delta\Gamma_{\text{MgCl}_2}^{\text{D}}$ , that is experimentally measured, in which case,<sup>9,36</sup>

$$\Delta\Gamma_{\text{MgCl}_2}^{\text{D}} = \frac{\partial(\Delta G_{\text{D}}/kT)}{\partial \ln(c_{\text{Mg}})} = \nu_{\text{Mg}} + \nu_{\text{Cl}(\text{Mg})} \quad (22)$$

where  $\nu_{\text{Cl}(\text{Mg})}$  is the “bound” fraction of chloride ions that were added as part of the magnesium salt. Although it is frequently assumed that  $\nu_{\text{Mg}}$  is the dominant contribution to  $\Gamma_{\text{MgCl}_2}$  for added  $\text{MgCl}_2$ , it should, once again, be realized that this ignores potentially important thermodynamic effects of added coions.<sup>9</sup>

As an example, the interaction of  $\text{Mg}^{2+}$  with linear polynucleotides, like poly(A · U) and DNA, is best described by an ensemble of ions under the influence of the electrostatic field of the RNA.<sup>9</sup> The interaction of  $\text{Mg}^{2+}$  with these systems has been characterized extensively in classical experiments.<sup>39</sup> For these systems, the stoichiometry of  $\text{Mg}^{2+}$  binding can be calculated using the NLPB equation. As shown in Figure 3a, calculations using the NLPB equation reproduce quite well the experimental  $\text{Mg}^{2+}$  binding isotherms for poly(A · U) without needing to use any fitting parameters.<sup>9</sup>

The  $\text{Mg}^{2+}$  binding isotherms for poly(A · U), shown as Scatchard plots in Figure 3b, illustrate two characteristic features of the ensemble: first, the extent of  $\text{Mg}^{2+}$  binding,  $\nu_{\text{Mg}}$ , decreases with increasing monovalent salt concentrations (i.e., the coupling between monovalent and divalent cations); and second,  $\text{Mg}^{2+}$  binding is highly anticooperative as evidenced by the curvature of the Scatchard plots (i.e., the coupling among bound divalent cations). Comparing the experimental data to the calculated curves in each of these plots shows that each of these phenomena can be satisfactorily explained by the ensemble description of binding arising from the NLPB equation.<sup>9</sup>

These calculations show that the higher charge of  $\text{Mg}^{2+}$  makes it more effective than  $\text{Na}^+$  in binding to nucleic acids for two reasons<sup>9</sup>: first,  $\text{Mg}^{2+}$  have a stronger coulombic attraction (compared to monovalent cations) to the polyion [i.e.,  $\Delta G_{\text{E-D}}$  favors  $\text{Mg}^{2+}$  binding, in Eq. (17)]; and second, binding of each divalent ion results in the entropically favorable “release” of 1.8 sodium ions [i.e., the change in  $\Delta G_{\text{org}}^{\text{Na}}$  favors  $\text{Mg}^{2+}$  binding, in Eq. (17)]. Nevertheless, as monovalent cations are added to solution, their local concentration around the polynucleotide increases resulting in the displacement of the  $\text{Mg}^{2+}$  ensemble. As expected, the competition between monovalent and divalent ions is such that 1.8 bound  $\text{Na}^+$  effectively displace a single bound  $\text{Mg}^{2+}$ .<sup>9</sup>

The NLPB model also shows how two related electrostatic phenomena give rise to the anticooperativity of binding.<sup>9</sup> First, the monovalent ion ensemble around the nucleic acid becomes progressively de-

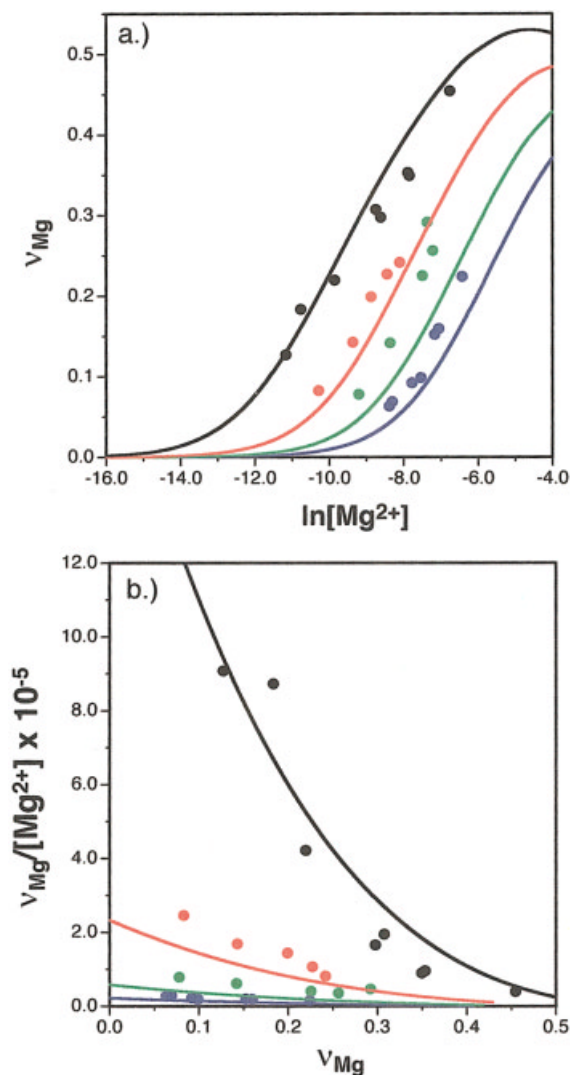


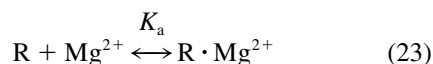
**FIGURE 3** (A) Magnesium binding isotherms for poly(A · U). The term  $\nu_{\text{Mg}}$  is the number of  $\text{Mg}^{2+}$  bound per nucleic acid charge. The filled circles are experimental data points taken from Krakauer.<sup>39</sup> The solid lines were calculated with the cylindrical NLPB equation using a one-dimensional finite difference algorithm in reciprocal space.<sup>9</sup> Each color represents a different  $\text{Na}^+$  concentration. Black:  $c_{\text{Na}}^{\text{b}} = 0.01\text{M}$ ; Red:  $c_{\text{Na}}^{\text{b}} = 0.029\text{M}$ ; Green:  $c_{\text{Na}}^{\text{b}} = 0.06\text{M}$ ; Blue:  $c_{\text{Na}}^{\text{b}} = 0.1\text{M}$ . (B) The corresponding Scatchard plots for  $\text{Mg}^{2+}$  binding to poly(A · U) (colors as above).

pleted as  $\text{MgCl}_2$  is added to solution. As a result, there is an incremental loss of free energy associated with the “release” of sodium ions,  $\Delta G_{\text{org}}^{\text{Na}}$ , at high  $\text{MgCl}_2$  concentrations. Second, the surrounding  $\text{Mg}^{2+}$  ensemble becomes more populated. As a result, the entropic cost of organizing additional magnesium ions around the RNA,  $\Delta G_{\text{org}}^{\text{Mg}}$ , becomes energetically more expensive; and to a lesser extent, the Coulombic repulsion among Mg ions, included in  $\Delta\Delta G_{\text{E-D}}$ , increases.

### The Interaction of Chelated $Mg^{2+}$ with the RNA.

As mentioned above, some  $Mg^{2+}$  interact with sites on the RNA where anionic ligands chelate the ion through strong Coulombic forces. In contrast to ions described by the PB ensemble, the strong attractive interactions involved in chelation disrupt ionic hydration. As noted above, dehydration or partial dehydration of an ion has a substantial energetic cost that must be explicitly treated.

We consider here only the case of a single chelated ion, although the formalism can be extended easily to treat chelation by multiple sites. The interaction of a single Mg ion can be described by the equilibrium reaction<sup>11</sup>:



where R is the folded RNA without any chelated  $Mg^{2+}$ ,  $R \cdot Mg^{2+}$  is the RNA with a single chelated  $Mg^{2+}$ , and  $K_a$  is the association constant for the reaction. We can define a “standard state” free energy for this reaction,  $\Delta G_S^\circ = -RT \ln K_a$ , which is the difference in chemical potential of the bound ( $R \cdot Mg^{2+}$ ) and free (R and  $Mg^{2+}$ ) species in a solution containing  $MgCl_2$ . For purely electrostatic interactions,  $\Delta G_S^\circ$  can be calculated using the NLPB equation as the difference in the electrostatic free energies of the bound and free species.<sup>11,35,36,40</sup> The “standard state” free energy  $\Delta G_S^\circ$  can be partitioned into several terms<sup>11</sup>:

$$\Delta G_S^\circ = \Delta G^{\text{elec}} + \Delta G_{Mg}^{\text{solv}} + \Delta G_{RNA}^{\text{solv}} + \Delta G_{RNA}^{\text{Na}} + \Delta G_{RNA}^{\text{Mg}} + \Delta G_{Mg}^{\text{trans}} \quad (24)$$

$\Delta G^{\text{elec}}$  is the electrostatic attraction of  $Mg^{2+}$  to the site (the “solvent-screened” Coulombic interaction free energy);  $\Delta G_{Mg}^{\text{solv}}$  is the dehydration free energy of the ion upon binding;  $\Delta G_{RNA}^{\text{solv}}$  is the dehydration free energy of the RNA site upon binding;  $\Delta G_{RNA}^{\text{Na}}$  is the free energy of displacing the bound ensemble of univalent salt and  $\Delta G_{RNA}^{\text{Mg}}$  is the corresponding free energy of displacing the bound ensemble of divalent salt from around the RNA upon site-binding (energetically coupling the chelated  $Mg^{2+}$  with the surrounding  $Mg^{2+}$  ensemble); and  $\Delta G_{Mg}^{\text{trans}}$  is the free energy associated with the loss of translational entropy upon binding. The binding free energy at an arbitrary  $MgCl_2$  concentration,  $c_{Mg}$ , is given by the Langmuir isotherm,

$$\Delta G_S = -kT \ln(1 + c_{Mg} \exp(-\Delta G_S^\circ/kT)) \quad (25)$$

which accounts for the concentration dependent contribution to binding at nonstandard states.

We assume here that differences in the electrostatic solvation free energies ( $\Delta G_{Mg}^{\text{solv}}$ ,  $\Delta G_{RNA}^{\text{solv}}$ ,  $\Delta G_{RNA}^{\text{Na}}$ , and  $\Delta G_{RNA}^{\text{Mg}}$ ) and attractive electrostatic free energy ( $\Delta G^{\text{elec}}$ ) are the primary determinants of chelation to a specific site. While other contributions like van der Waals interactions and changes in the conformational entropy of the RNA certainly influence binding, their energetic contribution is thought to be small compared to the overall electrostatic interaction of  $Mg^{2+}$  with the RNA.

The Born model is a very simple formalism to describe energetic changes associated with ionic dehydration upon binding.<sup>11</sup> In this model, ions are represented as spheres defined by their effective radii immersed in a dielectric continuum. The Born radii have a well-defined physical meaning related to the size of the solvent cavity formed by the ion.<sup>41–43</sup> The cost of dehydration in the Born model is determined by changes to the surrounding dielectric medium upon binding to the RNA. The Born model is very accurate and avoids the inherent complexity of modeling an explicit hydration layer.<sup>41,44</sup> Using such a model, the NLPB equation provides a physically reasonable description of chelation.<sup>11</sup>

The change in the number of bound Mg ions associated with chelation by a single site can be written in terms of a preferential interaction coefficient,<sup>28</sup>

$$\Delta \Gamma_{MgCl_2}^S = \frac{\partial(\Delta G_S^N/kT)}{\partial \ln[MgCl_2]} = (\nu_S + \Delta \nu_{Mg} + \Delta \nu_{Cl(Mg)}) \quad (26)$$

where  $\nu_S$  is the fractional occupancy of the chelated  $Mg^{2+}$  at its site; while  $\Delta \nu_{Mg}$  and  $\Delta \nu_{Cl(Mg)}$  refer to the change in the bound fraction of magnesium and chloride ions within the surrounding ensemble upon chelation to a specific site at a given  $MgCl_2$  concentration. An important feature of this equation is that the anticooperative energetic coupling between the chelated ion and the surrounding ensemble ( $\Delta G_{RNA}^{\text{Mg}}$ ) is also manifested as a stoichiometric coupling [ $\Delta \nu_{Mg}$  and  $\Delta \nu_{Cl(Mg)}$ ].

## A DESCRIPTION OF RNA FOLDING

### Unfolded States (U)

As noted above, RNA folding can be described as a hierarchical process that proceeds through intermediate states with increasing levels of secondary and



tertiary structure organization.<sup>12–14</sup> Under denaturing conditions, such as high temperature or low ionic strength, RNAs exist in an unfolded state, designated U. Though it may have some residual structure,<sup>45</sup> the U state is an ensemble of conformational microstates that persist as a set of extended single stranded conformations.<sup>46</sup> The energetics of the unfolded state are dominated by the interaction of various polar groups with the surrounding aqueous solvent, the strong electrostatic repulsion among the negatively charged phosphate groups, and the conformational entropy of the chain. Folding must overcome these energetic barriers.

### Intermediate States (I)

Under folding conditions (e.g., lower temperature and higher salt concentrations), the polynucleotide chain cooperatively folds into more compact structures. The initial stages of RNA folding lead to a compact, disordered intermediate state, designated I.<sup>15–17</sup> Rigorous high resolution models have not yet been developed that can treat either an unfolded or partially unfolded ensemble adequately. However, the I state can be described as a family of conformational microstates characterized predominantly by elements of double helical secondary structure, without any well-defined tertiary contacts. In fact, for most RNA molecules, more than half of all nucleotides can be found in standard A-form double helices.<sup>1,47</sup> These helical regions are structurally linked by hairpin loops, bulges, and internal loops.<sup>1,47</sup>

The stability of the I state is determined by base stacking and base pairing.<sup>12</sup> Though secondary structure is very stable (the standard free energy of folding,  $\Delta G_{\text{fold}}^{\circ}$ , is  $-1$  to  $-3$  kcal  $\cdot$  mol<sup>-1</sup> per nucleotide), the formation of secondary structure is accompanied by substantial energetic costs associated with the loss of conformational entropy and the increase in interphosphate coulombic repulsions.<sup>48</sup> Thus, as shown for the helix–coil transition of double-stranded polynucleotides, the formation of secondary structure is facilitated by both monovalent and divalent cations that reduce interphosphate Coulombic repulsions in solution.<sup>49–56</sup>

Mg<sup>2+</sup> binding to the I state must be calculated from the average electrostatic properties of the conformational ensemble. As mentioned above, the average properties of a nucleotide in the I state are governed primarily by short double helical elements of secondary structure. Based on this notion, the average electrostatic properties for a nucleotide in the I state ensemble can be calculated as an average over each position of the nucleotide in a single turn of a canonical A-form helix.<sup>28</sup> Such a model equally weights the

contributions of nucleotides in the middle of the duplex and those at the ends of a duplex, thus qualitatively accounting for the heterogeneous environments present in the I state. The Mg<sup>2+</sup> binding free energy per nucleotide is dominated by the interaction with negatively charged phosphate groups and does not depend strongly on nucleotide sequence.<sup>28</sup>

It is known that Mg<sup>2+</sup> interacts with double-helical nucleic acids as a delocalized “ion cloud” without chelation at specific sites.<sup>55</sup> These ions, therefore, can be treated simply as a Boltzmann weighted ensemble of the electrostatic potential. The partition function for Mg<sup>2+</sup> interactions with the I state,  $\xi_I$ , is entirely determined by this single class of ions,

$$\xi_I = \exp(-\Delta G_D^I/kT) \quad (27)$$

where it is presumed that the magnesium binding free energy to the I state,  $\Delta G_{\text{Mg}}^I$ , is equal to the interaction free energy of Mg<sup>2+</sup> ensemble with the RNA,  $\Delta G_D^I$ . The interaction of the ensemble with helical nucleic acids is determined by the charge of the ion and the magnitude of the surrounding electrostatic potentials. Ionic properties like size, electronegativity, and pK<sub>a</sub> only weakly affect binding. The linkage between Mg<sup>2+</sup> binding and secondary structure formation is governed by the Coulombic attraction of the ions to the higher charge density of double-helical structures in the I state relative to the U state. The higher ionic charge of the bound Mg<sup>2+</sup> makes them more effective than Na<sup>+</sup> in stabilizing secondary structures as discussed above. However, as expected, the interaction of low concentrations of magnesium with simple secondary structures is generally quite weak at physiological (0.1–0.2M) monovalent cation concentrations.<sup>9,39,57,58</sup>

Mg<sup>2+</sup> interaction with the I state has been measured directly only for yeast tRNA<sup>Phe</sup>. In this case, the interaction was studied at high temperature (45–70°C) to maintain the I state without tertiary structure formation. The experimental Mg<sup>2+</sup> binding isotherms, shown in Figures 4a and 4b, shows the characteristic monovalent salt dependence and anticooperativity for the interaction of the Mg<sup>2+</sup> ensemble with the RNA. Using the structural description of the I state discussed above, the NLPB model reproduces the experimentally measured stoichiometry of Mg<sup>2+</sup> binding (Figures 4a and 4b).<sup>28</sup> The calculations in Figure 5a show that the Mg<sup>2+</sup> ensemble interacts with the I state of the tRNA with a free energy,  $\Delta G_{\text{Mg}}^I$ , of just more than  $-4$  kcal  $\cdot$  mol<sup>-1</sup> at 0.1 mM MgCl<sub>2</sub> at 0.032M NaCl.<sup>28</sup> The energetics of the interaction recapitulate the patterns discussed for polynucleotides above.

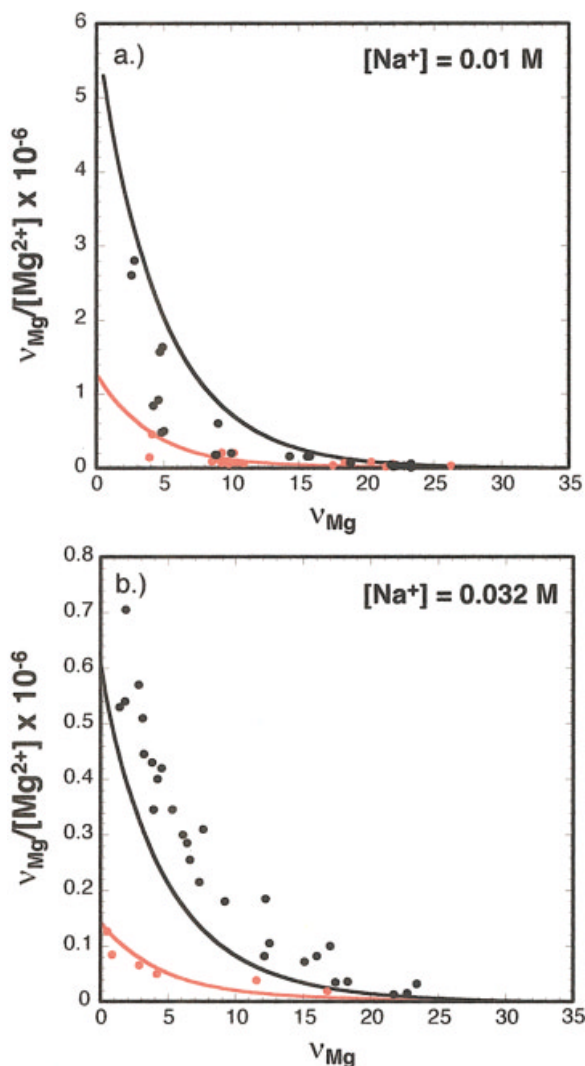


**FIGURE 4** Scatchard plots for  $\text{Mg}^{2+}$  binding to yeast  $\text{tRNA}^{\text{Phe}}$ . The term  $\nu_{\text{Mg}}$  is the number of bound  $\text{Mg}^{2+}$  per  $\text{tRNA}$ . The data points for the I state (red) and the N state (black) are taken from prior experimental work. The corresponding lines were calculated using the finite difference NLPB equation for the I and N states. (a)  $0.01\text{M}$  monovalent salt concentration, data from Ref. 57; (b)  $0.032\text{M}$  monovalent salt concentration, data from Ref. 58.

### Folded States (N)

As folding proceeds, the secondary structural elements of the I state assemble into a compact, native tertiary structure. The fully folded tertiary structure, designated N, is described by a small, well-defined ensemble of states. The average structure of the N state can be determined experimentally by traditional methods like x-ray crystallography and NMR spectroscopy. In most structure based thermodynamic models, it is assumed that the properties of the aver-

age structure represent the ensemble average. Thus, the thermodynamic properties of the N state are usually modeled directly from the average atomic resolution structure gleaned from high-resolution methods.<sup>59,60</sup>

Like secondary structure, tertiary structures are also stabilized by base stacking and base pairing interactions. Standard Watson–Crick pairing is accom-

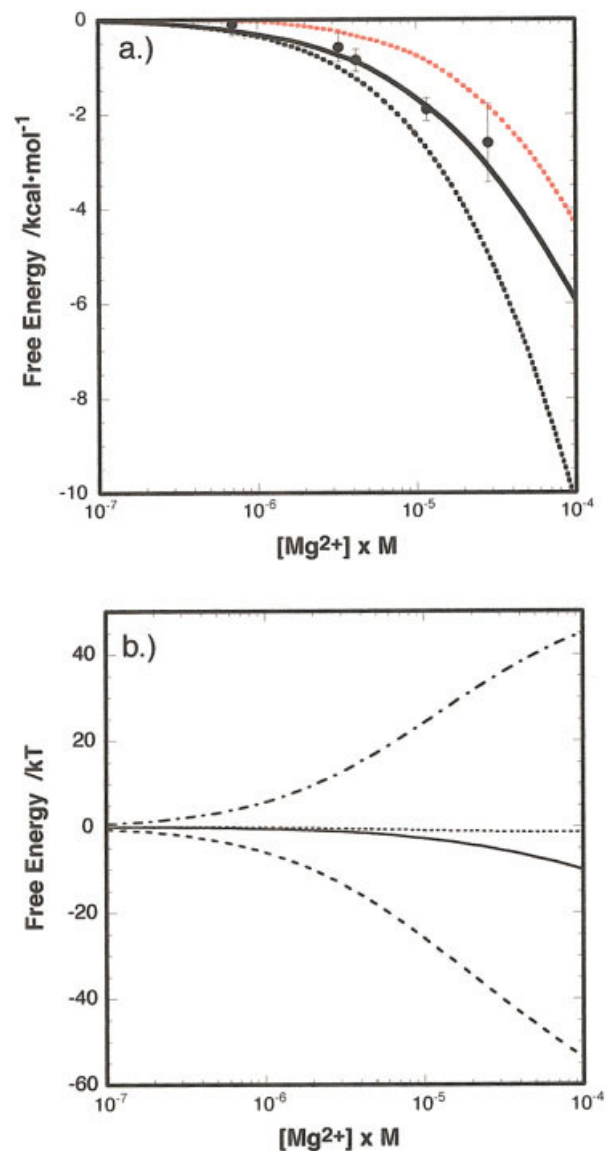


**FIGURE 5** The free energy contribution of  $\text{Mg}^{2+}$  binding to yeast  $\text{tRNA}^{\text{Phe}}$  folding at  $0.032\text{M}$  monovalent salt concentration. (A) Comparing the calculated value of  $\Delta\Delta G_{\text{Mg}}$  (—) to the experimental results (●) of Romer and Hach.<sup>58</sup> The plot includes values of  $\Delta G_{\text{Mg}}^{\text{N}}$  (····) and  $\Delta G_{\text{Mg}}^{\text{I}}$  (···). (B) The change in the free energy contributions to  $\text{Mg}^{2+}$  binding upon RNA folding. (—)  $\Delta\Delta G_{\text{Mg}}$ , (····)  $\Delta\Delta G_{\text{E-D}}$ , (---)  $\Delta\Delta G_{\text{org}}^{\text{Na}}$ , and (-·-·-·)  $\Delta\Delta G_{\text{org}}^{\text{Mg}}$ .

panied by a number of other interactions that optimize van der Waals contacts, hydrophobic interactions, and hydrogen bonding between secondary structure elements.<sup>1,61</sup> For folding to occur, the energetic advantage gained by these interactions must outweigh the disadvantage of losing conformational entropy. The overall stability of tertiary structure varies from about  $-1$  to  $-10$  kcal  $\cdot$  mol<sup>-1</sup> depending on the identity of the RNA and solution conditions.<sup>13</sup>

Two strong electrostatic energies tend to disrupt the RNA tertiary structure, the desolvation energy of partially burying charged phosphate groups within the folded structure and the Coulombic repulsion among phosphate groups juxtaposed by folding. However, salts added to solution substantially attenuate these energetic costs and stabilize the folded structure of most RNA molecules. Though monovalent cations can both alleviate the cost of burying phosphates<sup>62</sup> and reduce electrostatic repulsions between phosphates,<sup>4-8</sup> divalent cations play an especially important role in the electrostatic stability of most RNA molecules. Mg<sup>2+</sup> binding, in particular, is strongly coupled to tertiary structure formation for most RNAs and favors the folding reaction.<sup>4</sup> Thus, while Mg<sup>2+</sup> has little effect on the thermal denaturation of tRNA secondary structure at physiological (0.1–0.2M) monovalent cation concentrations, added Mg<sup>2+</sup> strongly stabilizes the tertiary structure.<sup>63,64</sup>

The strong attractive interactions between Mg<sup>2+</sup> and the N state involves both the surrounding ensemble of ions as well as any ions chelated by the RNA.<sup>11,28</sup> The overall partition function for Mg<sup>2+</sup> interactions with the N state can, therefore, be written<sup>11,28</sup>

$$\xi_N = \exp(-\Delta G_B^N/kT)[1 + c_{Mg} \exp(-\Delta G_S^N/kT)] \quad (28)$$

From this equation, the overall magnesium binding free energy to the N state,  $\Delta G_{Mg}^N$ , is

$$\Delta G_{Mg}^N = -kT \ln \xi_N = \Delta G_D^N + \Delta G_S^N \quad (29)$$

where  $\Delta G_D^N$  is the interaction free energy of the Mg<sup>2+</sup> ensemble and  $\Delta G_S^N$  is the interaction free energy of specifically chelated ions. In the next section, we will explore Mg<sup>2+</sup> interactions with the N state of three different RNA systems.

## Mg<sup>2+</sup> BINDING TO THE N STATE

### Transfer RNA

The N state of most RNA molecules is structurally more complex than simple elements of double-helical

structure. As shown for the N state of yeast tRNA<sup>Phe</sup> in Figure 6b, the irregular shape of the RNA surface of these compact structures can result in pockets of highly negative electrostatic potential where ions within the surrounding ensemble are localized.<sup>10,30,65</sup> It is, of course, these localized ions that are energetically most interesting. However, as noted previously, the energetic properties of individual ions near the RNA are tightly coupled to those of other surrounding ions and cannot be determined without accounting for the interactions among all the ions.

Our current understanding of ionic interactions with folded RNA molecules, in both thermodynamic and structural terms, is largely based on classical studies of tRNA.<sup>66</sup> The importance of cations in the folding of yeast tRNAs was evident nearly 30 years ago when it was shown that Mg<sup>2+</sup> could restore the amino acid acceptor activity of denatured tRNA.<sup>67</sup> Soon afterward it was shown that a number of univalent and divalent cations could effectively renature tRNA.<sup>68</sup> Systematic thermal melting profiles under a variety of ionic conditions characterized the influence of both univalent and divalent salts on tRNA conformational equilibria.<sup>8</sup> In these studies, Mg<sup>2+</sup> was shown to strongly stabilize the native tertiary structure of tRNA.

The interaction of Mg<sup>2+</sup> with several tRNA molecules has been studied under solution conditions that uncouple binding from structural transitions in the RNA.<sup>57,58,69-72</sup> For example, the interaction of Mg<sup>2+</sup> with the N state of yeast tRNA<sup>Phe</sup> has been studied at low temperature and moderate univalent salt concentrations to uncouple binding from the RNA folding.<sup>57,58,71,72</sup> Such studies are absolutely required to study ion binding independently of the confounding energetic effects of RNA folding.<sup>28,66</sup> Unfortunately, most studies of Mg<sup>2+</sup> binding to RNA do not uncouple ion binding from RNA folding.<sup>4,28</sup>

The experimental Mg<sup>2+</sup> binding isotherms for the N state of yeast tRNA<sup>Phe</sup><sup>9,10</sup> are qualitatively similar to those of linear polynucleotides and I state discussed above. The Scatchard plots in Figures 4a and 4b show the characteristic monovalent salt dependence and anticooperatively of Mg<sup>2+</sup> binding. Comparing the experimental data to the calculated curves in these plots shows that Mg<sup>2+</sup> binding to yeast tRNA<sup>Phe</sup> are well described as an ensemble of ions distributed according to a Boltzmann weighted averages of the mean electrostatic potential around the RNA, without invoking any specifically chelated ions.<sup>10</sup>

The energetic features of Mg<sup>2+</sup> interactions with the N state of tRNA are also qualitatively similar to the energetic features of Mg<sup>2+</sup> interactions with linear polynucleotides.<sup>10</sup> That is to say, the interaction is

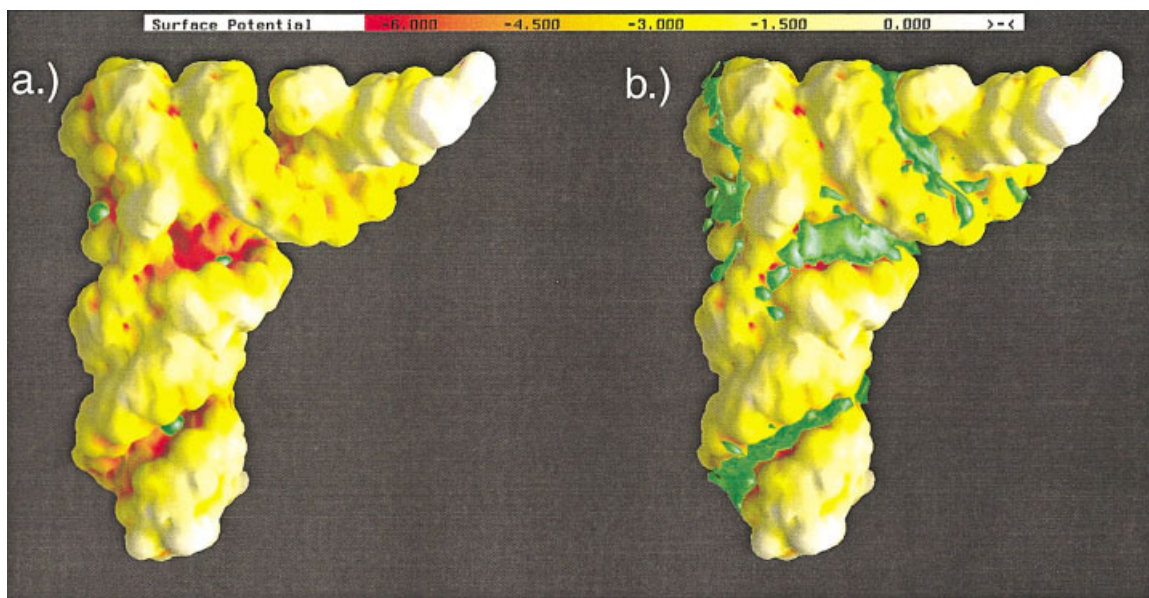


**FIGURE 6** (A) The electrostatic surface potential of on one face of yeast tRNA<sup>Phe</sup> calculated at  $c_{\text{Na}}^{\text{b}} = 0.01M$  and  $c_{\text{Mg}}^{\text{b}} = 0.02M$  (corresponding to the crystallization conditions of the monoclinic form). The crystallographically observed  $\text{Mg}^{2+}$  in the monoclinic form<sup>84</sup> are shown as green spheres. Their correspondence to regions of highly negative electrostatic potentials (red) is seen. The surface potential scale is in units of  $kT/e$ . (B) the 3.0M three-dimensional  $\text{Mg}^{2+}$  isoconcentration contour around yeast tRNA<sup>Phe</sup> shown in green. The surrounding ensemble of  $\text{Mg}^{2+}$  accumulates in surface cavities with high negative surface charge densities. The figure was rendered using GRASP.<sup>85</sup>

driven by the favorable Coulombic attraction of the ions with the RNA [ $\Delta G_{\text{E-D}}$  in Eq. (6)] and the favorable entropic free energy of  $\text{Na}^+$  release ( $\Delta G_{\text{org}}^{\text{Na}}$ ). At 0.1 mM  $\text{MgCl}_2$ ,  $\text{Mg}^{2+}$  binds to the N state with a free energy of about  $-10$  kcal/mol 0.032M monovalent salt concentration (Figure 5a). This binding free energy arises entirely from the interaction of the surrounding  $\text{Mg}^{2+}$  ensemble with the RNA.

The NLPB model suggests a relationship between the ensemble of ions surrounding the RNA in solution and ions observed in crystallographic and NMR structures of the N state.<sup>10,11</sup> According to the NLPB model, the extent to which Mg ions are localized to any particular region of the RNA depends on the local surface charge density of the nucleic acid. Even in relatively featureless linear polynucleotides, like poly(A · U) or DNA, many of the bound Mg ions within the surrounding ensemble accumulate in the major and minor grooves, and are confined to a relatively small volume near the nucleic acid.<sup>73</sup> Yet the energetics of these ions are best described as a part of a thermally fluctuating ensemble that interacts with the strong anionic field around the nucleic acid via long-range Coulombic interactions alone.

For yeast tRNA<sup>Phe</sup> the bound  $\text{Mg}^{2+}$  can also be described in this way. The irregular shape of the

molecular surface of tRNA results in the localized accumulation of Mg ions in pockets of very high negative electrostatic potential (Figure 6b). As shown in Figure 6a, the experimentally observed ions are also found in these potential wells.<sup>10</sup> Thus, the NLPB model suggest that the ions observed in the x-ray crystallographic structures of the tRNA are highly localized ions that are part of the surrounding ensemble. These Mg ions are seen in high potential regions simply because they have a high probability of being found there. We note, however, that these localized ions must exchange with bulk solution such that any perturbations to their hydration layer at a particular location is energetically insignificant in terms of the ensemble; on average, the chemical potential of these ions is characterized by the bulk aqueous state. The correlation between crystallographically observed  $\text{Mg}^{2+}$  and the electrostatic potential have been presented for several other RNAs, including the P4–P6 domain of the *Tetrahymena* group I intron, the loop E fragment of the 5S RNA, and the hammerhead ribozyme.<sup>30,65,74</sup>

### RNA Hairpins from the Group I Intron

The P5 helix<sup>74</sup> and the P5b stem loop<sup>75</sup> from the P4–P6 domain of the *Tetrahymena thermophila*

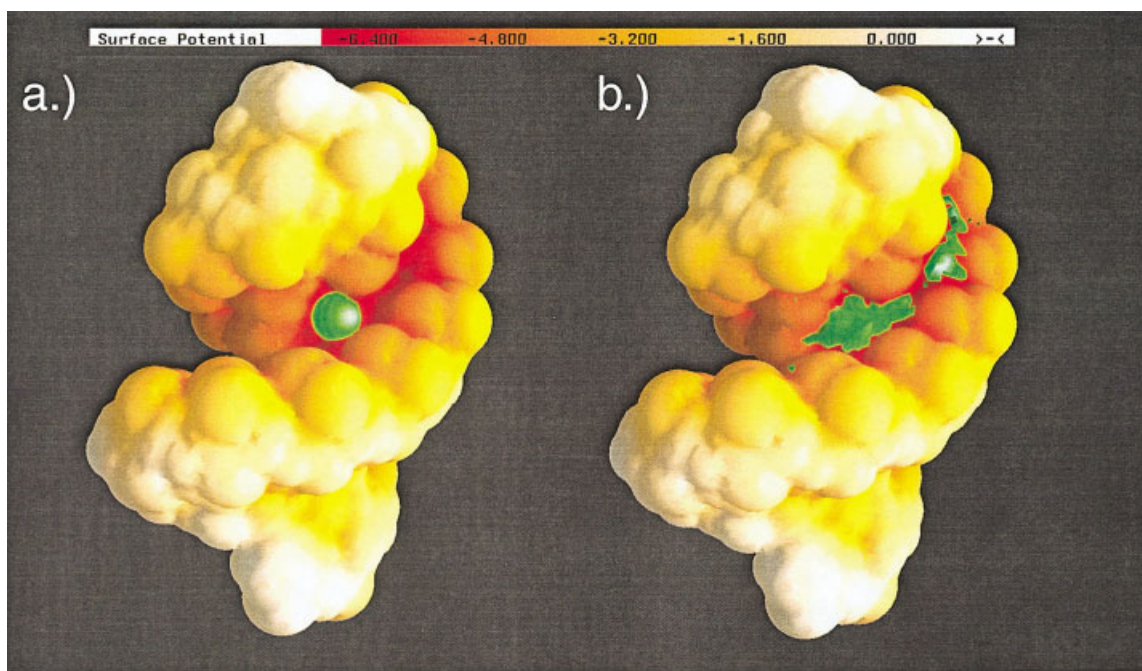


**FIGURE 7** (A) The electrostatic potential mapped onto the solvent accessible surface of the P5 helix<sup>75</sup> calculated at 0.1M univalent salt concentration and 0.001M bulk magnesium concentration. The experimentally observed metal ion is shown as a green sphere in a pocket of highly negative potential (red). (B) The 4.5M three-dimensional isoconcentration contour of  $Mg^{2+}$  around the RNA is shown in green. The correspondence of the high concentration region of the surrounding ensemble to the observed ion is seen. The surface potential scale is in units of  $kT/e$ . The figure was rendered using the program GRASP.<sup>85</sup>

group I intron provide models for the interaction of magnesium with simple folded RNA motifs.  $Mg^{2+}$  binding to these simple RNA hairpins was initially characterized using proton NMR spectroscopy of cobalt (III) hexamine as an analogue of solvated magnesium.<sup>74,75</sup> These studies were able to localize a metal ion in a region of highly negative electrostatic potential in the major groove of each of these hairpins (Figure 7a). It was postulated that a single  $Mg^{2+}$  was chelated at this location and was important for RNA stability.<sup>74,75</sup> The NLPB model has been used to explore the energetics of  $Mg^{2+}$  binding to the presumed binding site in the context of the overall  $Mg^{2+}$  induced stabilization of the RNA.<sup>11</sup>

For the P5 helix and the P5b stem loop,  $Mg^{2+}$  is strongly attracted to the RNA grooves, as expected. The electrostatic potential at the observed site in the major groove is between about  $-6$  to  $-7 kT/e$ . These values are typical of those found in the grooves of double helical nucleic acids.<sup>10,65,76,77</sup> This negative potential provides a strong driving force for the chelation of  $Mg^{2+}$  by the RNA, as reflected by the large coulombic attraction free energy,  $\Delta\Delta G^{elec}$ . However, this attractive free energy is counterbalanced by the

large cost of dehydrating the  $Mg^{2+}$  ( $\Delta\Delta G_{Mg}^{solv}$ ) and the RNA site ( $\Delta\Delta G_{RNA}^{solv}$ ,  $\Delta\Delta G_{RNA}^{Na}$ ).

For both hairpins, the enormous cost of dehydrating the  $Mg^{2+}$  itself outweighs the attractive free energy. For these hairpins, it is important to realize that the localized ions have a completely intact inner hydration layer. The term  $\Delta\Delta G_{Mg}^{solv}$  arises primarily from the displacement of water molecules in outer hydration shells. Perturbing these outer shell waters costs more than  $35 \text{ kcal} \cdot \text{mol}^{-1}$ . This large free energy change is consistent with experimental findings showing that removal of even a single one of these water molecules can cost up to  $10 \text{ kcal} \cdot \text{mol}^{-1}$ .<sup>32</sup> For the P5 helix and the P5b stem loop, the accompanying cost of dehydrating the partially charged groups in the RNA binding site ( $\Delta\Delta G_{RNA}^{solv}$ ) is relatively small, but significant.

The formation of the chelated  $Mg^{2+}$ -RNA complex is also strongly opposed by the displacement of sodium from around the nucleic acid ( $\Delta\Delta G_{RNA}^{Na}$ ). This effect, generally seen in the interaction of charged ligands with nucleic acids, is due to the repulsion and displacement of monovalent ion ensemble by the chelated  $Mg^{2+}$ .<sup>23,36,40,78</sup> It is a “desolvation penalty”

arising from the loss of favorable electrostatic interactions between the univalent ion and the RNA.<sup>23</sup> The NLPB equation provides a very accurate estimate of this term.<sup>78</sup> In most cases, the free energy of chelation will depend critically on  $\Delta\Delta G_{\text{RNA}}^{\text{Na}}$ . For example, for the P5b stem loop, the magnitude of  $\Delta\Delta G_{\text{RNA}}^{\text{Na}}$  is substantially larger than  $\Delta\Delta G^{\text{elec}}$  at 0.1M bulk sodium concentration. The analogous contribution arising from the displacement of ions within bound  $\text{Mg}^{2+}$  ensemble,  $\Delta\Delta G_{\text{RNA}}^{\text{Mg}}$ , couples the interaction of the chelated ion to the  $\text{Mg}^{2+}$  ensemble. At the high monovalent ion concentrations used in many experiments,  $\Delta\Delta G_{\text{RNA}}^{\text{Mg}}$  is relatively small (Table I).

Chelation is also opposed by the loss of translational entropy of the  $\text{Mg}^{2+}$ ,  $\Delta\Delta G_{\text{Mg}}^{\text{trans}}$ . This term, which is estimated to be about 1 to 3 kcal/mol,<sup>79</sup> has a small but potentially important contribution to binding. Changes in the conformational entropy of the RNA due to  $\text{Mg}^{2+}$  binding are extremely difficult to estimate,<sup>80</sup> but are likely to weakly oppose binding.

For the P5 helix and the P5b stem loop, the overall free energy change,  $\Delta G_{\text{S}}^{\text{c}}$ , strongly opposes chelation of  $\text{Mg}^{2+}$  in the major groove. This is because the favorable electrostatic interaction between the  $\text{Mg}^{2+}$  and the RNA ( $\Delta\Delta G^{\text{elec}}$ ) cannot overcome the large cost of desolvating the ion and the nucleic acid (i.e.,  $\Delta\Delta G_{\text{Mg}}^{\text{solv}}$  and  $\Delta\Delta G_{\text{RNA}}^{\text{Na}}$ ). In contrast, the surrounding ensemble of Mg ions strongly stabilizes the folded hairpins at physiological  $\text{Mg}^{2+}$  concentrations. At 1 mM  $\text{MgCl}_2$  concentration and 0.1M NaCl concentration, the calculated value of  $\Delta G_{\text{D}}$  is  $-1.6 \text{ kcal} \cdot \text{mol}^{-1}$ .<sup>11</sup> The experimentally observed  $\text{Mg}^{2+}$  association constants for each hairpin are at least  $1-1.5 \times 10^2 \text{ M}^{-1}$ ,<sup>74</sup> and are therefore, readily explained by  $\Delta G_{\text{D}}$  alone.

As discussed for tRNA, the ensemble of magnesium ions preferentially accumulates in the major groove of the hairpin and stabilizes the folded hairpin by interacting most strongly with pockets of negative potential formed by the irregular shape of the molecular surface. Three dimensional isoconcentration contours showing the regions of highest  $\text{Mg}^{2+}$  accumulation are shown in Figure 7b. The isoconcentration contour represents the time averaged spatial distribution of  $\text{Mg}^{2+}$  around the RNA. Comparing Figures 7a and 7b, the region of ionic accumulation corresponds to the experimentally observed metal ion, similar to what has been found for yeast tRNA<sup>Phe</sup>.<sup>10</sup>

### A 23S rRNA Fragment

A 58-nucleotide fragment (nucleotides 1051–1108) derived from the *E. coli* large subunit rRNA folds into an extraordinarily compact tertiary structure.<sup>81</sup> Inter-

estingly, a four-nucleotide segment of backbone (residues 1070–1073) is completely buried within the “core” of the RNA. As a result, folding must overcome the energetic cost of burying these charged phosphate groups, as well as the Coulombic repulsion among the closely packed charges in the N state. Not surprisingly, thermal denaturation experiments show that this RNA fragment requires both monovalent and divalent ions to fold.<sup>6,19,82,83</sup> Analyses of the experimental data suggest that the N state of the rRNA fragment is stabilized by one selectively bound  $\text{Mg}^{2+}$  and another much less selective class of Mg ions at 1.6M monovalent salt concentration.<sup>82</sup>

At least ten Mg ions can be seen in the refined crystallographic structure of the RNA shown in Figure 8a.<sup>62</sup> Again, all of these metal ions are found in regions of highly negative electrostatic potential. Like the RNA hairpins described above, most of these ions lie in the grooves of the RNA where the electrostatic potential is between about  $-2$  to  $-9 \text{ kT/e}$  (Figure 8b).<sup>62</sup> The energetics of  $\text{Mg}^{2+}$  binding to these sites is found to be qualitatively quite similar to that observed for the hairpin structures. That is to say,  $\Delta\Delta G^{\text{elec}}$  cannot overcome the large cost associated with  $\Delta\Delta G_{\text{Mg}}^{\text{solv}}$  and  $\Delta\Delta G_{\text{RNA}}^{\text{Na}}$ . As a result, chelation of  $\text{Mg}^{2+}$  at these specific locations is negligible. The sites where these metal ions are observed correspond to electronegative pockets where there is a high probability of finding an individual ion in the bound  $\text{Mg}^{2+}$  ensemble due to their high local concentrations (Figure 8c).<sup>62</sup> The energetics of these ions are best described as an ensemble governed by the electrostatic potential around the RNA.

However, the electrostatic potentials at two sites are an order of magnitude larger than at other locations. As shown in Figures 8a and 8b, one of these ions is near the anionic phosphate oxygen of A1073 and the O4 position of U1094 (this ion is designated 167) while the other is chelated by the anionic phosphate oxygens of A1070 and C1072 (this ion is designated 163). These two sites are located within an interhelical cleft where the sugar–phosphate backbone is buried within the RNA. In this region, the electrostatic field is focused to form two deep electronegative pockets where the Mg ions are found (Figure 8b). For each of these ions, the Coulombic attraction to the site provides a strong driving force for binding as reflected by  $\Delta\Delta G^{\text{elec}}$ . However, at site 163, the large cost of displacing both inner and outer layer waters from around the deeply buried  $\text{Mg}^{2+}$  ( $\Delta\Delta G_{\text{Mg}}^{\text{solv}}$ ) together with the repulsion of the monovalent ion atmosphere,  $\Delta\Delta G_{\text{RNA}}^{\text{Na}}$ , outweigh  $\Delta\Delta G^{\text{elec}}$  to oppose binding at the site. In contrast, the ion at site 167 is able to exploit the large electrostatic potential in the

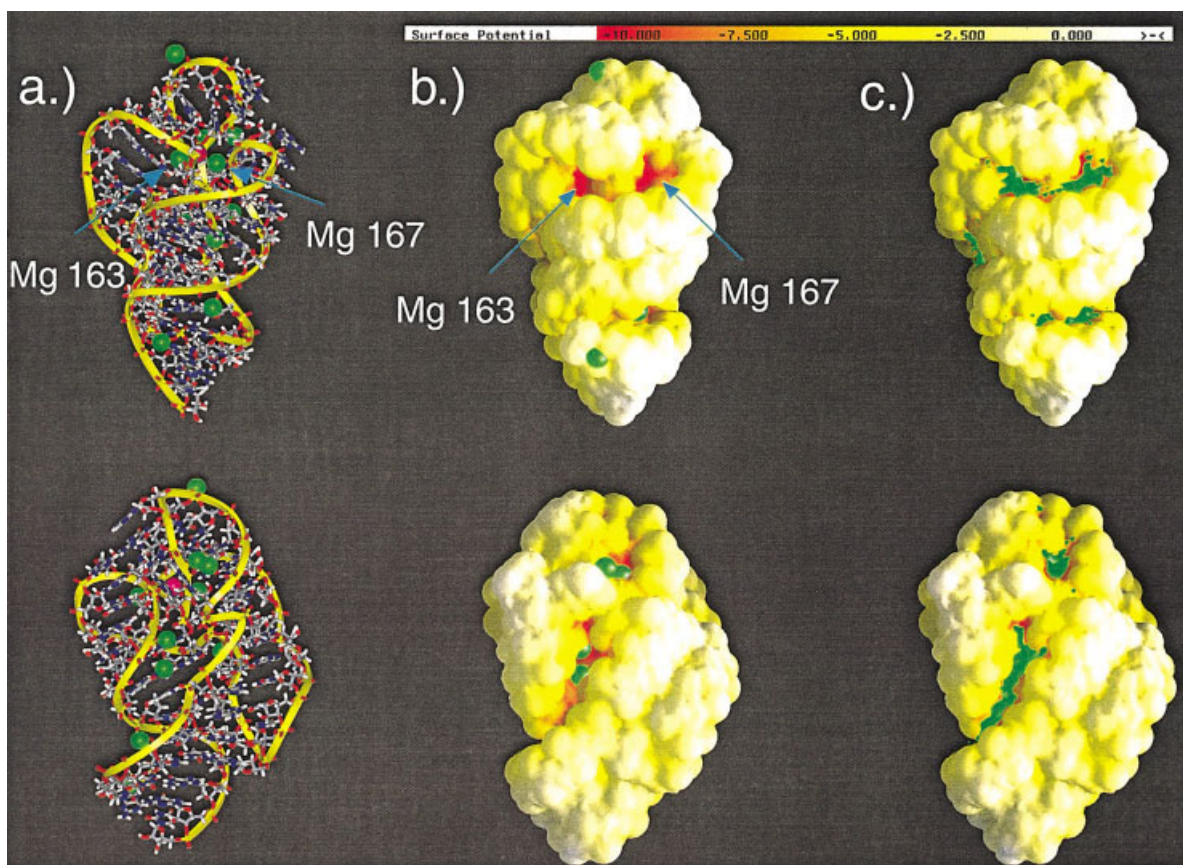


**FIGURE 8** (A) An overview of the metal ion positions in the refined crystal structure of the 58-nucleotide rRNA fragment. The observed magnesium ions are shown as green spheres; a bound potassium ion is magenta. (B) The electrostatic potential mapped onto the solvent-accessible surface of the RNA calculated at 0.15M univalent salt concentration and 0.001M bulk magnesium concentration. The surface potential scale is in units of  $kT/e$ . The two high potential regions corresponding to Mg 163 and 167 are seen in the upper panel. (C) The 4.5M three-dimensional isoconcentration contour of  $Mg^{2+}$  around the RNA is shown in green. The correspondence of the crystallographically observed magnesium ions to high potential regions where the surrounding ensemble accumulates with high concentrations is again apparent. The figures were rendered using the program GRASP.<sup>85</sup>

cleft by remaining more solvent exposed thereby reducing  $\Delta\Delta G_{Mg}^{solv}$ , a strategy that has been noted for other nucleic acid binding ligands.<sup>78</sup> Thus, of the many Mg ions observed around the RNA, only the one at position 167 has a favorable free energy associated with chelation,  $\Delta G_S$ .

Surprisingly, the calculations show that the surrounding ensemble of Mg ions also remain associated with the N state of the rRNA fragment, even at 1.6M univalent salt concentration.<sup>11</sup> This finding is qualitatively consistent with the two classes of binding sites that are suggested by the experimental  $Mg^{2+}$  binding isotherms.<sup>82</sup> The interaction free energy of the  $Mg^{2+}$  ensemble ( $\Delta G_D$ ) and the chelated  $Mg^{2+}$  ( $\Delta G_S$ ) are compared in Figure 9a. At 1 mM bulk  $Mg^{2+}$  concentration, the chelated ion at position 167 binds to the RNA with a free energy of  $-0.8 \text{ kcal} \cdot \text{mol}^{-1}$  while

the surrounding ensemble of Mg ions binds with a free energy of about  $-0.3 \text{ kcal} \cdot \text{mol}^{-1}$ . As the  $Mg^{2+}$  concentration is increased,  $\Delta G_D$  quickly becomes the larger contributor to RNA stability.

### THE LINKAGE BETWEEN $Mg^{2+}$ BINDING AND RNA FOLDING

The linkage between tertiary structure folding and magnesium ion binding is shown schematically by the thermodynamic cycle in Figure 1. As stated at the outset, to understand why RNA folding in the presence of  $Mg^{2+}$  is more favorable than in its absence, we must understand why  $Mg^{2+}$  binding to the N state is so much more favorable than to the I state. That is to say, in Figure 1, in order to understand why  $\Delta G_F^{Mg}$

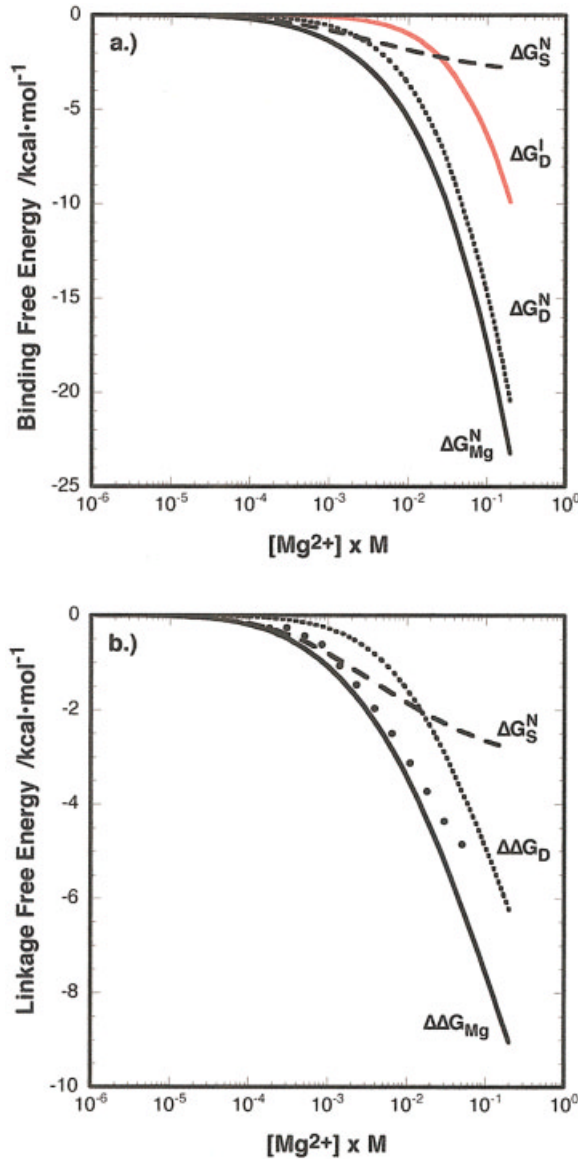


**FIGURE 9** The free energy contribution of Mg<sup>2+</sup> binding to folding of the 58-nucleotide rRNA fragment at 1.6M monovalent salt concentration. (A) The free energy contributions of Mg<sup>2+</sup> binding to the N and I states. The plot includes the following:  $\Delta G_{Mg}^N$ ; the total Mg<sup>2+</sup> binding free energy to the N state;  $\Delta G_S^N$ , the free energy of Mg<sup>2+</sup> chelation to the N state;  $\Delta G_D^N$ , the interaction free energy of the Mg<sup>2+</sup> ensemble with the N state;  $\Delta G_D^I$ , the interaction free energy of the Mg<sup>2+</sup> ensemble with the I state. Note  $\Delta G_D^I$  equals  $\Delta G_{Mg}^I$ . (B) Comparing the calculated value of  $\Delta \Delta G_{Mg}$  to the experimental results<sup>82</sup> (●). The plot includes the free energy of Mg<sup>2+</sup> chelation,  $\Delta G_S^N$ , and the change in the interaction free energy of the Mg<sup>2+</sup> ensemble upon folding,  $\Delta \Delta G_D$ .

$< \Delta G_F^O$ , we must explain why  $\Delta G_{Mg}^N < \Delta G_{Mg}^I$ . In this section, we explore this linkage for two systems: yeast tRNA<sup>Phe</sup>, in which Mg<sup>2+</sup> behaves strictly as an en-

semble to stabilize the RNA; and the 58-nucleotide fragment derived from the *E. coli* large subunit rRNA, in which Mg<sup>2+</sup> acts, in part, as an ensemble, but also by chelation to a specific site to stabilize the RNA.

## Transfer RNA

As we have described above, the experimentally observed Mg<sup>2+</sup> binding isotherms for the I and N states of yeast tRNA<sup>Phe</sup> (Figures 5a and 5b) are simply explained by an ensemble of ions that are distributed according to a Boltzmann weighted average of the mean electrostatic potential around the RNA. Moreover, as shown in Figure 5a, the calculated Mg<sup>2+</sup> binding free energy to the N state,  $\Delta G_{Mg}^N$ , is much more favorable than the corresponding Mg<sup>2+</sup> binding free energy for the I state,  $\Delta G_{Mg}^I$ .<sup>28</sup> The difference between these two curves is the contribution of Mg<sup>2+</sup> binding to the RNA folding free energy,  $\Delta \Delta G_{Mg}$ . Comparing the calculated<sup>28</sup> and experimental<sup>58</sup> values of  $\Delta \Delta G_{Mg}$ , the NLPB equation provides an accurate description of the measured thermodynamic linkage between Mg<sup>2+</sup> binding and yeast tRNA<sup>Phe</sup> folding (Figure 5a). Thus, we can use the NLPB model to present a meaningful picture of how the surrounding Mg<sup>2+</sup> ensemble promotes tRNA folding.

We have presented RNA folding as a hierarchical process proceeding from elements of extended secondary structure in the I state to more compact domains of tertiary structure in the N state. The surrounding ensemble of Mg ions interact with secondary structure through long-range electrostatic interactions with the backbone phosphate groups. Thus, 0.1 mM MgCl<sub>2</sub> added to 0.032M NaCl stabilizes the I state by  $-4.2 \text{ kcal} \cdot \text{mol}^{-1}$  at 25°C (Figure 5a). As the RNA folds, the Mg<sup>2+</sup> strongly interacts with elements of compact tertiary structure by accumulating in surface cavities that have a high negative electrostatic potential. These localized Mg ions ameliorate the unfavorable electrostatic free energy by reducing the local electrostatic potentials and displacing Na<sup>+</sup> into bulk solution. Thus, for yeast tRNA<sup>Phe</sup>, adding 0.1 mM MgCl<sub>2</sub> to 0.032M NaCl stabilizes the N state by  $-10.1 \text{ kcal} \cdot \text{mol}^{-1}$  at 25°C (Figure 5a). Consequently, 0.1 mM MgCl<sub>2</sub> added to solution favors the tertiary folding transition of yeast tRNA<sup>Phe</sup> by nearly  $-6 \text{ kcal} \cdot \text{mol}^{-1}$  under these solution conditions (Figure 5a). It must be emphasized again that, in the NLPB model, the preferential interaction of Mg<sup>2+</sup> with tRNA tertiary structure is fully described as an ensemble of ions governed by the electrostatic potentials.

A more detailed energetic analysis suggests how the surrounding Mg<sup>2+</sup> ensemble promotes tRNA fold-



ing. As described in Eq. (17), the change in the magnesium binding free energy upon tRNA folding,  $\Delta\Delta G_{\text{Mg}}$ , can be partitioned into three contributions arising from the interaction of the ensemble with the RNA:  $\Delta\Delta G_{\text{E-D}}$ , the change in the electrostatic stress of the system upon folding;  $\Delta\Delta G_{\text{org}}^{\text{Mg}}$ , the entropic free energy of reorganizing the bound  $\text{MgCl}_2$  ensemble upon folding; and  $\Delta\Delta G_{\text{org}}^{\text{Na}}$ , the entropic free energy of reorganizing the bound  $\text{NaCl}$  ensemble upon folding. The surrounding ensemble of ions preferentially interacts with the N state to alleviate the enormous electrostatic stress arising from the closely packed phosphate groups. As shown in Figure 5b, NLPB calculations show that at 0.032M  $\text{NaCl}$  concentration, the electrostatic stress of folding is largely compensated by monovalent ions so that the addition of more than 0.1 mM  $\text{MgCl}_2$  causes very little change in  $\Delta\Delta G_{\text{E-D}}$ . In other words, at these concentrations,  $\text{Na}^+$  and  $\text{Mg}^{2+}$  are equally effective in reducing the electrostatic stress of the system. However, the association of each additional  $\text{Mg}^{2+}$  within the ensemble results in the stoichiometric “release” of 1.9 Na ions upon folding.<sup>28</sup> Consequently, as shown in Figure 5b, the folding reaction in the presence of  $\text{Mg}^{2+}$  is greatly favored by the entropic free energy of “releasing” these Na ions ( $\Delta\Delta G_{\text{org}}^{\text{Na}}$ ) compared to entropic cost of organizing the ensemble of bound  $\text{Mg}^{2+}$  ( $\Delta\Delta G_{\text{org}}^{\text{Mg}}$ ). That is, the effect of the surrounding  $\text{Mg}^{2+}$  ensemble of RNA folding is almost entirely determined by a purely entropic phenomenon arising from the higher charge on each  $\text{Mg}^{2+}$  compared to corresponding  $\text{Na}^+$  particles. A very similar phenomenon has been described previously in the context of counterion condensation theory.<sup>55</sup> However, in NLPB theory, counterion “release” is an electrostatic phenomenon arising from the global redistribution of ions.<sup>9,23,40</sup>

### The 23S rRNA Fragment

As discussed above, two distinct types of bound  $\text{Mg}^{2+}$  interact with N state of the 58 nucleotide fragment of the *E. coli* large subunit rRNA, a single chelated ion along with the surrounding ensemble of ions. Thus, the folding reaction is linked to both of these types of  $\text{Mg}^{2+}$  binding. Like tRNA, the rRNA fragment folds into a compact tertiary structure with regions of very high negative potential that preferentially interact with the surrounding ensemble of ions. In addition, folding creates a specific site that chelates  $\text{Mg}^{2+}$  and additionally stabilizes the tertiary structure. The contribution of  $\text{Mg}^{2+}$  binding to the RNA folding free energy,  $\Delta\Delta G_{\text{Mg}}$ , calculated using the NLPB equation<sup>28</sup> closely approximates the experimental data<sup>82</sup> at 1.6M monovalent salt concentration (Figure

9b). In these calculations,  $\Delta\Delta G_{\text{Mg}}$  is calculated as the sum of contributions from the interaction of the surrounding ensemble with the RNA,  $\Delta\Delta G_{\text{D}}$ , and the chelation of  $\text{Mg}^{2+}$  to specific sites,  $\Delta G_{\text{S}}^{\text{N}}$ . These two terms are also plotted in the Figure 9b.

It is very important to realize that ion binding is an electrostatic exchange reaction governed by the requirement for electroneutrality of the system. Ion binding is *not* simply determined by mass action. Under different ionic conditions, the free energy of the system is optimized by different stoichiometries of monovalent ions bound as an ensemble, monovalent ions chelated by specific sites, divalent ions bound as an ensemble, and divalent ions chelated by specific sites. However, the net charge of the system (RNA and salts) must always be zero. Thus, at low  $\text{Mg}^{2+}$  concentrations,  $\Delta G_{\text{S}}^{\text{N}}$  makes a larger magnesium-dependent contribution to RNA folding than  $\Delta\Delta G_{\text{D}}$ , because of the strong coulombic attraction between  $\text{Mg}^{2+}$  and its site (Figure 9b). However, chelation to a specific site necessarily displaces or “releases” ions from within the bound ensembles of monovalent and divalent ions around the nucleic acid (reflected by  $\Delta\Delta G_{\text{org}}^{\text{Na}}$  and  $\Delta\Delta G_{\text{org}}^{\text{Mg}}$ ). At higher  $\text{Mg}^{2+}$  concentrations  $\Delta\Delta G_{\text{D}}$  predominates (Figure 9b) because of the very favorable electrostatic free energy of “releasing” ions within the tightly bound ensemble of monovalent ions upon folding. However, the interaction of the  $\text{Mg}^{2+}$  ensemble is also anticooperatively coupled to chelation (given by  $\Delta\Delta G_{\text{RNA}}^{\text{Mg}}$ ) and influences the occupancy of the site.<sup>28</sup> Understanding the electrostatic interplay among these different classes of ions is crucial to understanding the linkage between ion binding and RNA folding. We have shown here that the NLPB model is a simple way to describe this linkage in accordance with the available experimental data.

### CONCLUSIONS

We have presented a theoretical model for understanding how  $\text{Mg}^{2+}$  binding is coupled to RNA folding. This model, based on the NLPB equation, describes how  $\text{Mg}^{2+}$  binds and stabilizes specific RNA structures. In this model, most of the ions surrounding an RNA behave as a thermally fluctuating ensemble distributed according to a Boltzmann weighted averages of the mean electrostatic potential around the RNA. However, in some cases, individual Mg ions may shed some of their surrounding waters to optimize their Coulombic interactions with the RNA. The large free energies associated with these processes are not adequately described by the simple ensemble description, so that these chelated ions must be explic-

itly treated. The NLPB model provides a quantitative physical description of these processes.

The surrounding ensemble of  $Mg^{2+}$  weakly stabilizes secondary structure through long-range electrostatic interactions with the backbone phosphate groups. These ions promote tertiary structure folding by strongly interacting with regions of high negative electrostatic potential created by tertiary structure formation. In contrast, chelation of  $Mg^{2+}$  by a folded RNA is relatively uncommon because of the large desolvation penalties. However, in special cases, like the 58-nucleotide rRNA fragment, chelation of  $Mg^{2+}$  in pockets on the RNA surface with extraordinarily high electrostatic potential provides an important, favorable driving force for the folding reaction. Importantly, the NLPB model provides a quantitative method to describe the electrostatic interplay among these different classes of ions that affect RNA folding.

This work was supported by Howard Hughes Medical Institute Physician Postdoctoral Fellowship to VKM and by NIH grant GM58545.

## REFERENCES

- Moore, P. B. *Annu Rev Biochem* 1999, 68, 287–300.
- Ferre-D'Amare, A. R.; Doudna, J. A. *Annu Rev Biophys Biomol Struct* 1999, 28, 57–73.
- Caprara, M. G.; Nilsen, T. W. *Nature Struct Biol* 2000, 7, 831–833.
- Misra, V. K.; Draper, D. E. *Biopolymers (Nucleic Acid Sci)* 1998, 48, 113–135.
- Draper, D. E.; Misra, V. K. *Nature Struct Biol* 1998, 5, 927–930.
- Wang, Y.-X.; Lu, M.; Draper, D. E. *Biochemistry* 1993, 32, 12279–12282.
- Basu, S.; Rambo, R. P.; Strauss-Soukup, J.; Cate, J. H.; Ferre-D'Amare, A. R.; Strobel, S. A.; Doudna, J. A. *Nature Struct Biol* 1998, 5, 986–992.
- Cole, P. E.; Yang, S. K.; Crothers, D. M. *Biochemistry* 1972, 23, 4358–4368.
- Misra, V. K.; Draper, D. E. *J Mol Biol* 1999, 294, 1135–1147.
- Misra, V. K.; Draper, D. E. *J Mol Biol* 2000, 299, 813–825.
- Misra, V. K.; Draper, D. E. *Proc Natl Acad Sci USA* 2001, 98, 12456–12461.
- Brion, P.; Westhof, E. *Annu Rev Biophys Biomol Struct* 1997, 26, 113–127.
- Draper, D. *Trends Biochem Sci* 1996, 21, 145–149.
- Tinoco, I.; Bustamante, C. *J Mol Biol* 1999, 293, 271–281.
- Russel, R.; Millett, I. S.; Doniach, S.; Herschlag, D. *Nature Struct Biol* 2000, 7, 367–370.
- Buchmueller, K. L.; Webb, A. E.; Richardson, D. A.; Weeks, K. M. *Nature Struct Biol* 2000, 7, 362–366.
- Fang, X. W.; Littrell, K.; Yang, X.; Henderson, S. J.; Siefert, S.; Thiagarajan, P.; Pan, T.; Sosnick, T. R. *Biochemistry* 2000, 39, 11107–11113.
- Hill, T. L. *Cooperativity Theory in Biochemistry, Steady State and Equilibrium Systems*; Springer-Verlag: New York, 1985.
- Laing, L. G.; Gluick, T. C.; Draper, D. E. *J Mol Biol* 1994, 237, 577–587.
- Draper, D. E.; Gluick, T. C. *Methods Enzymol* 1995, 259, 281–305.
- Eisenberg, H. *Biological Macromolecules and Polyelectrolytes in Solution*; Clarendon: Oxford, 1976.
- Bockris, J. O. M.; Reddy, A. K. N. *Modern Electrochemistry. I*; Plenum Press: New York, 1970; Vol I.
- Sharp, K. A.; Friedman, R. A.; Misra, V.; Hecht, J.; Honig, B. *Biopolymers* 1995, 36, 245–262.
- Anderson, C. F.; Record, M. T. *Annu Rev Phys Chem* 1995, 46, 657–700.
- Fang, X.; Pan, T.; Sosnick, T. R. *Biochemistry* 1999, 38, 16840–16846.
- Heilman-Miller, S. L.; Thirumalai, D.; Woodson, S. A. *J Mol Biol* 2001, 306, 1157–1166.
- Celander, D. W.; Cech, T. R. *Science* 1991, 251, 401–407.
- Misra, V. K.; Draper, D. E. *J Mol Biol* 2002, 317, 509–523.
- Chen, S. W.; Honig, B. *J Phys Chem B* 1997, 101, 9113–9118.
- Hermann, T.; Westhof, E. *Structure* 1998, 6, 1303–1314.
- Burgess, J. *Metal Ions in Solution*; Wiley & Sons: New York, 1978.
- Peschke, M.; Blades, A. T.; Kebarle, P. *J Phys Chem A* 1998, 102, 9978–9985.
- Eisenman, G. *Biophys J* 1962, 2, 259–323.
- Eisenman, G.; Horn, R. *J Membr Biol* 1983, 76, 197–225.
- Gilson, M. K.; Honig, B. *Proteins Struct Funct Genet* 1988, 4, 7–18.
- Sharp, K. A. *Biopolymers* 1995, 36, 227–243.
- Sharp, K. A.; Honig, B. *J Phys Chem* 1990, 94, 7684–7692.
- Stigter, D.; Dill, K. A. *Biophys J* 1996, 71, 2064–2074.
- Krakauer, H. *Biopolymers* 1971, 10, 2459–2490.
- Misra, V. K.; Sharp, K. A.; Friedman, R. A.; Honig, B. *J Mol Biol* 1994, 238, 245–263.
- Rashin, A. A.; Honig, B. *J Phys Chem* 1985, 89, 5588.
- Roux, B.; Yu, H. A.; Karplus, M. *J Phys Chem* 1990, 94, 4683–4688.
- Babu, C. S.; Lim, C. *Chem Phys Lett* 1999, 310, 225–228.
- Jayaram, B.; Fine, R.; Sharp, K.; Honig, B. *J Phys Chem* 1989, 93, 4320–4327.
- Saenger, W. *Principles of Nucleic Acid Structure*; Springer-Verlag: New York, 1984.
- Sen, S.; Nilsson, L. *J Am Chem Soc* 2001, 123, 7414–7422.

47. Hermann, T.; Patel, D. J. *J Mol Biol* 1999, 294, 829–849.
48. Burkard, M. E.; Turner, D. H.; Tinoco, I., Jr., *The Interactions that Shape RNA Structure*; Gesteland, R. F., Cech, T. R., Atkins, J. F., Eds.; Cold Spring Harbor Laboratory Press: Cold Spring Harbor, NY, 1999; pp 233–264.
49. Porschke, D. *Biophys Chem* 1976, 4, 383–394.
50. Porschke, D. *Nucleic Acids Res* 1979, 6, 883–898.
51. Cowan, J. A.; Huang, H.-W.; Hsu, L.-Y. *J Inorg Biochem* 1993, 52, 121–129.
52. Buckin, V.; Tran, H.; Morozov, V.; Marky, L. A. *J Am Chem Soc* 1996, 118, 7033–7039.
53. Duguid, J.; Bloomfield, V.; Benevides, J.; Thomas, G. J. *Biophys J* 1993, 65, 1916–1928.
54. Skerjanc, J.; Strauss, U. P. *J Am Chem Soc* 1968, 90, 3201–3205.
55. Manning, G. S. *Q Rev Biophys* 1978, 11, 179–246.
56. Manning, G. S. *Biophys Chem* 1977, 7, 141–145.
57. Rialdi, G.; Levy, J.; Biltonen, R. *Biochemistry* 1972, 11, 2472–2479.
58. Romer, R.; Hach, R. *Eur J Biochem* 1975, 55, 271–284.
59. Sharp, K. A.; Honig, B. *Annu Rev Biophys Biomol Struct* 1990, 19, 301–332.
60. Honig, B.; Nicholls, A. *Science* 1995, 268, 1144–1149.
61. Doherty, E. A.; Batey, R. T.; Masquida, B.; Doudna, J. A. *Nature Struct Biol* 2001, 8, 339–343.
62. Conn, G. L.; Gittis, A. G.; Lattman, E. L.; Misra, V. K.; Draper, D. E., submitted.
63. Crothers, D. M.; Cole, P. E.; Hilbers, C. W.; Shulman, R. G. *J Mol Biol* 1974, 87, 63–88.
64. Stein, A.; Crothers, D. M. *Biochemistry* 1976, 15, 160–168.
65. Chin, K.; Sharp, K. A.; Honig, B.; Pyle, A. M. *Nature Struct Biol* 1999, 6, 1055–1061.
66. Schimmel, P. R.; Redfield, A. G. *Ann Rev Biophys Bioeng* 1980, 9, 181–221.
67. Lindahl, T.; Adams, A.; Fresco, J. R. *Proc Natl Acad Sci USA* 1966, 55, 941–948.
68. Fresco, J. R.; Adams, A.; Ascione, R.; Henley, D.; Lindahl, T. *Cold Spring Harbor Symp Quant Biol* 1966, 31, 527–537.
69. Bina-Stein, M.; Stein, A. *Biochemistry* 1976, 15, 3912–3917.
70. Stein, A.; Crothers, D. M. *Biochemistry* 1976, 15, 157–160.
71. Maglott, E. J.; Deo, S. S.; Przykorska, A.; Glick, G. D. *Biochemistry* 1998, 37, 16349–16359.
72. Privalov, P. L.; Filimonov, V. V. *J Mol Biol* 1978, 122, 447–464.
73. Robinson, H.; Gao, Y.; Sanishvili, R.; Joachimiak, A.; Wang, A. H.-J. *Nucleic Acids Res* 2000, 28, 1760–1766.
74. Colmenarejo, G.; Tinoco, I. *J Mol Biol* 1999, 290, 119–135.
75. Kieft, J. S.; Tinoco, I. J. *Structure* 1997, 5, 713–721.
76. Jayaram, B.; Sharp, K. A.; Honig, B. *Biopolymers* 1989, 28, 975–993.
77. Sharp, K. A.; Honig, B.; Harvey, S. C. *Biochemistry* 1990, 29, 340–346.
78. Misra, V. K.; Honig, B. *Proc Natl Acad Sci USA* 1995, 92, 4691–4695.
79. Amzel, L. M. *Proteins* 1997, 28, 144–149.
80. Reyes, C. M.; Kollman, P. A. *J Mol Biol* 2000, 297, 1145–1158.
81. Conn, G. L.; Draper, D. E.; Lattman, E. E.; Gittis, A. G. *Science* 1999, 284, 1171–1174.
82. Bukhman, Y. V.; Draper, D. E. *J Mol Biol* 1997, 273, 1020–1031.
83. Laing, L. G.; Draper, D. E. *J Mol Biol* 1994, 237, 560–576.
84. Westhof, E.; Sundaralingam, M. *Biochemistry* 1986, 25, 4868–4878.
85. Nicholls, A.; Sharp, K. A.; Honig, B. *Proteins Struct Funct Genet* 1991, 11, 281–296.